Physics – Uspekhi **50** (10) 1053 – 1077 (2007)

REVIEWS OF TOPICAL PROBLEMS PACS numbers: **76.60. – k**, **82.56. – b**, **87.61. – c**

Nuclear magnetic resonance in condensed matter

A G Lundin, V E Zorin

DOI: 10.1070/PU2007v050n10ABEH006308

Contents

Abstract. The basic ideas and principles of condensed-matter nuclear magnetic resonance are reviewed. The potential of the method for studying the structure and properties of liquids and solids is examined. The state of the art of the method and its associated problems are discussed.

A G Lundin Siberian State Technological University, prosp. Mira 82, Krasnoyarsk, Russian Federation
Tel. (7-391) 227 39 25
Fax (7-391) 266 03 90
E-mail: arlund@rol.ru
V E Zorin Durham University, University Science Laboratories, South Road, Durham, DH13LE, United Kingdom
E-mail: vadim.zorin@durham.ac.uk

Received 6 December 2006, revised 21 May 2007
Uspekhi Fizicheskikh Nauk **177** (10) 1107 – 1132 (2007)
DOI: 10.3367/UFNr.0177.200710c.1107
Translated by V Kisin; edited by A M Semikhatov

1. Introduction

An important discovery was made in 1946: two groups of American scientists were independently able to observe nuclear magnetic resonance (NMR) in condensed media [1 – 4]. The leaders of these groups (Felix Bloch and Edward Mills Purcell) were awarded the 1952 Nobel Prize in Physics. [1] It would have been difficult to predict at the time of the discovery that NMR was to become one of the most efficient physical methods for studying the structure and properties of

[1] The method of nuclear magnetic resonance later received three more Nobel Prizes: the 1991 Nobel Prize in Chemistry to Richard Ernst for his contributions to the development of the methodology of high-resolution NMR spectroscopy, the 2002 Nobel Prize in Chemistry to Kurt Wuthrich for the development of methods for the identification and structural analysis of biological macromolecules, and the 2003 Nobel Prize in Physiology and Medicine to Paul C Lauterbur and Sir Peter Mansfield for their discoveries concerning magnetic resonance imaging.

matter in different phase states, finding wide application in many areas in industry and agriculture, geophysics and geology, biophysics and medical sciences.

NMR was first observed in experiments in solid samples and it became clear very soon that the resonating nuclei constitute sensitive probes incorporated into solids and respond in very subtle ways to various changes in the matter surrounding them: its structure, chemical bonding, isotopic composition, temperature, pressure, and so forth. Nevertheless, progress in NMR techniques for solid-state research in the first 20 years was considerably slower than in the case of liquids.

When liquids are studied using high-resolution techniques, even very small changes in the chemical environment of nuclei are revealed, owing to the narrow natural width of resonance lines. This feature transformed the NMR method into one of the most efficient techniques of structural analysis of organic and other molecules, allowed its application to the study of the kinetics of chemical reactions, isomerism, hydrogen bonding, and the electron structure of molecules, and to solving other fundamental problems in chemistry and chemical physics. By virtue of the obvious feedback, this aspect inevitably impacted the method itself: elaborate equipment was designed and mass produced, measurement techniques were improved, the main fields of application of NMR to liquids were defined, and extensive special literature was published, including a number of monographs [5–8].

The situation in solid-state NMR in the same period was not so favorable because spectra were typically unresolved. The main obstacle here was a high dipole–dipole interaction between nuclei, which masked subtler effects caused by electron shielding, structural nonequivalence of nuclei, etc.

Things started to change radically after 1966, when pulse methods of line narrowing were proposed to eliminate the dipole–dipole interaction [9, 10], which launched the era of 'high-resolution NMR in solids.' Numerous experimental methods for manipulating nuclear spin systems were developed; they allowed recording NMR spectra with nucleus–nucleus, electron–nucleus, quadrupole, and other interactions 'turned on,' 'turned off,' or transformed to suit experimenters' wishes.

As a result, no integrated research project aimed at a specific material can progress without using nuclear magnetic resonance. NMR is now a natural component of the research, study, and control of various processes and materials in industry, practical medicine, physics, chemistry, and other fields of science and technology. But NMR work in Russia lags considerably behind in scale and level of research and applications compared to most developed countries. We also note that reviews in Russian are almost nonexistent. At the same time, a large number of original publications, reviews, and monographs on the subject are appearing outside Russia. Some of these monographs are published in Russian after an inevitable delay. But the original review papers — the most rapid response to the current status and to the hot issues in the NMR field — can so far be read only in English (see, e.g., [11–14]).

The need to have a review paper in Russian is dictated, in our opinion, by the fact that the rapid progress in sophisticated and difficult to understand NMR techniques, which greatly extend the potential of NMR applications in condensed media for various purposes, is continuing. This is especially true for NMR in solid systems; in this review, we intend to describe this aspect in more detail.

To facilitate better understanding of the underlying ideas and principles of NMR, we attempt as much as possible to give explanations citing the earliest original publications, where the material is typically presented clearly and in sufficient detail. This approach allows us to trace the development of the NMR techniques and theory without going into excessive detail. The review ends with characterizing the current status and problems concerning NMR. The review puts special stress on presenting the physical aspects of NMR; applications are considered in less detail.

2. Elementary condition of resonance

Protons and neutrons in atomic nuclei have a spin. Many nuclei also have a mechanical angular momentum $\mathbf{J}$ and a magnetic moment $\boldsymbol{\mu}$; the vectors $\mathbf{J}$ and $\boldsymbol{\mu}$ can be assumed parallel, and we therefore write

$$\boldsymbol{\mu} = \gamma \mathbf{J}\,, \tag{2.1}$$

where γ is the gyromagnetic ratio. In quantum mechanics, the operator $\mathbf{J}$ is related to the spin operator $\mathbf{I}$ by

$$\mathbf{J} = \hbar \mathbf{I}\,, \tag{2.2}$$

where $\hbar = h/2\pi$ is the reduced Planck constant. The eigenvalues of the operator $\mathbf{I}^2$ are $I(I+1)$, where I is the spin number, or simply spin. The magnetic moment $\boldsymbol{\mu}$ in a magnetic field $\mathbf{B}$ has the energy $E = -\boldsymbol{\mu}\mathbf{B}$, known as the Zeeman energy. The corresponding Hamiltonian

$$H = -\boldsymbol{\mu}\mathbf{B} \tag{2.3}$$

for a constant magnetic field $\mathbf{B}_0$ (we assume it to be directed along the z axis of the laboratory frame) can be written as

$$H = -\mu_z B_0 = -\gamma \hbar B_0 I_z\,, \tag{2.4}$$

where I_z is the operator of the z projection of spin. I_z can take one of the $2I+1$ values

$$m = I, I-1, \ldots, -I\,, \tag{2.5}$$

and therefore the possible energy values corresponding to Hamiltonian (2.4) are

$$E_m = -\gamma \hbar B_0 m\,. \tag{2.6}$$

As follows from (2.6), the energy difference ΔE between neighboring levels ($\Delta m = \pm 1$) is

$$\Delta E = \gamma \hbar B_0\,. \tag{2.7}$$

for any I.

If a system of noninteracting magnetic nuclei placed in a constant magnetic field is irradiated with a high-frequency (RF) electromagnetic field of frequency ν whose energy quanta coincide with ΔE, i.e.,

$$\hbar\omega = 2\pi\hbar\nu = \gamma \hbar B_0 \tag{2.8}$$

(ω is the angular frequency), then this field induces resonance transitions between levels. Quantum mechanical selection rules dictate that transitions are only possible between

neighboring levels, i.e., if $\Delta m = \pm 1$; Eqn (2.8) then implies that the resonance frequency is

$$\omega_0 = \gamma B\,. \tag{2.9}$$

The resonance frequency in Hz is defined by

$$\nu_0 = \frac{\gamma B_0}{2\pi}\,. \tag{2.10}$$

It is convenient to express the quantity $\gamma/2\pi$ in MHz T^{-1}. For protons, $\gamma/2\pi = 42.58$ MHz T^{-1}, and, for example, the resonance frequency in the field $B_0 = 11$ T is $\nu_0 = 468.4$ MHz.

3. Magnetic properties of nuclei

The spin of an isotopic nucleus with an even number Z of protons and an even number M of neutrons is always zero. As a result, NMR cannot be observed with nuclei such as ^{12}C, ^{16}O, and ^{32}S, because they have $I = 0$. The other group is formed of nuclei containing even Z and odd M or vice versa, odd Z and even M. All these nuclei have half-integral spins, e.g., ^{1}H, ^{19}F ($I = 1/2$), ^{7}Li, ^{23}Na ($I = 3/2$), ^{17}O, ^{27}Al ($I = 5/2$). And finally, nuclei with an odd number of protons and odd number of neutrons have an integral spin: ^{2}H, ^{14}N ($I = 1$), ^{10}B ($I = 3$), ^{50}V ($I = 6$).

However, even though even–even nuclei have no spin, it is still possible to observe NMR in practically all elements of the periodic table. For instance, resonance is usually observed in carbon using the ^{13}C isotope, in oxygen using ^{17}O, etc.

4. Energy absorption and spin-lattice relaxation

We let N_+ denote the number of spins at the lower level of a two-level system containing N nuclei with spin $I = 1/2$, and N_- denote that at the upper level, with $N = N_+ + N_-$; the ratio of populations at these levels is given by the Boltzmann factor

$$\frac{N_+}{N_-} = \exp\frac{\Delta E}{kT}\,, \tag{4.1}$$

where k is the Boltzmann constant and T is the absolute temperature. With the exception of the lowest accessible temperatures ($T \sim 1$ K), the ratio $\gamma\hbar B_0/kT$ in nuclear magnetic resonance is very low, and hence the ratio N_+/N_- differs from unity insignificantly. For instance, this ratio for protons at 300 K in a 10 T field is $\gamma\hbar B_0/kT \approx 10^{-4}$ (maximum γ among nuclei that are encountered most in NMR), and therefore

$$\frac{N_+}{N_-} \approx 1 + \frac{\gamma\hbar B_0}{kT} \approx 1 + 10^{-4}\,. \tag{4.2}$$

As the RF field of a resonance frequency interacts with matter, its quanta of energy $\Delta E = \hbar\omega$ induce transitions from the lower to the upper level (absorbing energy from the field), and reverse transition (releasing energy). The probability w of transitions per unit time (Einstein's coefficient) is the same in both directions of transition. However, owing to the small but finite excess of spins at the lower level, the number of upward transitions per unit time exceeds the number of transitions in the reverse direction, which results in absorption of energy of the RF field and in gradual equalization of level populations. If we introduce the quantity $n = N_+ - N_-$ (the difference between level populations), we can show (see, e.g., [15]) that

$$n = n_0 \exp(-2Pt)\,, \tag{4.3}$$

where n_0 is the value of n at $t = 0$ and P is the probability of the ac-field-induced transition between neighboring levels. It follows that owing to the alternating field, n tends to zero with time, the energy absorption terminates, and 'saturation' sets in. The interaction between the spins and the 'lattice' (defined as the matter incorporating the resonating nuclei regardless of whether it is a solid, liquid, or even gas) acts against this saturation. If spins are not aligned at the very beginning and there is no RF field, then turning on a constant magnetic field leads to the Boltzmann population difference setting in, as a result of the spin-lattice interaction:

$$n = n_0 = \frac{N\gamma\hbar B_0}{kT}\,. \tag{4.4}$$

When the RF field is switched on, the nuclear magnetization of a sample increases with time as

$$n = n_0\left[1 - \exp\left(-\frac{t}{T_1}\right)\right]. \tag{4.5}$$

The quantity $T_1 = 1/2w$ with the dimension of time, determining the rate at which the difference between level populations sets in due to the spin–lattice interaction, is known as the spin–lattice relaxation time. In real experimental conditions, the two competing processes — the saturation caused by the alternating RF field that tends to reduce n to zero and the spin–lattice relaxation that tends to produce the equilibrium population difference n_0 — produce a quasi-equilibrium spin distribution over levels. We then have

$$n = \frac{n_0}{1 + 2PT_1}\,. \tag{4.6}$$

Formula (4.6) makes it easy to analyze different situations depending on P, which is well known from elementary quantum theory to be proportional to the squared amplitude of the RF field [16] and to T_1.

We note that if the RF field is high and $T_2 \ll T_1$, which in the solid state holds virtually always, it is possible to define the 'spin temperature' T_S [8], which is in general higher than the lattice temperature:

$$\frac{N_+}{N_-} = \exp\left(\frac{N\gamma\hbar B_0}{kT_S}\right). \tag{4.7}$$

If the populations are equal ($N_+/N_- = 1$), the state is characterized by an infinitely high spin temperature.

5. System of spins in constant and alternating magnetic fields

Widely used along with the quantum mechanical theory of NMR is the classical resonance theory, because a number of characteristic features of NMR are obtained in a simpler and clearer way using the classical approach. We know that a change in angular moment must be equal to the applied momentum of external forces [17]. In the case of a spin with the moment $\mathbf{J} = \hbar\mathbf{I} = \boldsymbol{\mu}/\gamma$ in a constant magnetic field $\mathbf{B}_0$, this gives

$$\frac{\mathrm{d}\mathbf{J}}{\mathrm{d}t} = [\boldsymbol{\mu}\mathbf{B}_0] \tag{5.1}$$

or

$$\frac{\mathrm{d}\boldsymbol{\mu}}{\mathrm{d}t} = \gamma\,[\boldsymbol{\mu}\mathbf{B}_0]\,. \tag{5.2}$$

Rewriting this in projections onto coordinate axes, we find

$$\frac{\mathrm{d}\mu_x}{\mathrm{d}t} = \gamma\,(\mu_y B_z - \mu_z B_y) \tag{5.3}$$

(the expressions for $\mathrm{d}\mu_y/\mathrm{d}t$ and $\mathrm{d}\mu_z/\mathrm{d}t$ differ only in a cyclic transposition of coordinate indices). If the z axis is chosen parallel to B_0, then $B_z = B_0$ and $B_x = B_y = 0$. It is then easily established that

$$\frac{\mathrm{d}^2\mu_x}{\mathrm{d}t^2} + \gamma^2 B_0^2 \mu_x = 0\,. \tag{5.4}$$

This is a differential equation of free oscillations with the frequency $\omega_0 = \gamma B_0$. Taking into account that $\mathrm{d}\mu_z/\mathrm{d}t = 0$ (i.e., $\mu_z = \text{const}$), this implies that the projection of $\boldsymbol{\mu}$ onto the xy plane remains constant in magnitude and rotates counterclockwise for positive γ with the so-called Larmor frequency $\omega_0 = \gamma B_0$, which coincides with (2.9).

We now assume that in addition to a constant field B_0, there is also an alternating field in the plane perpendicular to B_0,

$$\mathbf{B}_1 = \mathbf{i}B_1 \cos\omega t - \mathbf{j}B_1 \sin\omega t\,. \tag{5.5}$$

The net field then equals

$$\mathbf{B} = B_1\,(\mathbf{i}\cos\omega t - \mathbf{j}\sin\omega t) + \mathbf{k}B_0\,, \tag{5.6}$$

where $\mathbf{i}$, $\mathbf{j}$, $\mathbf{k}$ are unit vectors of the coordinate axes. To clarify the behavior of the net magnetic moment vector $\mathbf{M} = \sum_i \boldsymbol{\mu}_i$, it is convenient to use a coordinate system rotating around the z axis with the frequency $\boldsymbol{\omega}$ in the same sense as $\mathbf{B}_1(t)$. The vector $\mathbf{B}_1$ is at rest in the rotating coordinate system.

If the axis of rotating coordinate system points along $\mathbf{B}_1$, then, as shown, e.g., in [18], we have

$$\frac{\mathrm{d}\boldsymbol{\mu}}{\mathrm{d}t} = \left[\boldsymbol{\mu},\, \gamma\left\{\left(B_0 - \frac{\omega}{\gamma}\right)\mathbf{k} + B_1\mathbf{i}\right\}\right] = \gamma\,[\boldsymbol{\mu}\mathbf{B}_{\mathrm{eff}}]\,, \tag{5.7}$$

where $\mathbf{B}_{\mathrm{eff}} = \mathbf{k}\,(B_0 - \omega/\gamma) + \mathbf{i}B_1$.

A comparison of (5.7) with (5.2) shows that the magnetic moment in the rotating frame moves as if it were under the effect of the effective magnetic field $\mathbf{B}_{\mathrm{eff}}$: it precesses around $\mathbf{B}_{\mathrm{eff}}$ with the angular frequency $\boldsymbol{\omega}_{\mathrm{eff}} = \gamma\mathbf{B}_{\mathrm{eff}}$ (Fig. 1a). If the alternating field frequency equals the Larmor frequency, then $\boldsymbol{\omega}_0 = -\gamma\mathbf{B}_0$ and $\mathbf{B}_{\mathrm{eff}} = \mathbf{i}B_1$, because the vector $\boldsymbol{\omega}$ is antiparallel to $\mathbf{B}_0$ (Fig. 1b), and hence the magnetic moment $\boldsymbol{\mu}$ precesses at the exact resonance around the x' axis of the rotating frame with the frequency $\boldsymbol{\omega}_1 = \gamma\mathbf{B}_1$. This frequency is typically much lower than $\omega_0 = \gamma\mathbf{B}_0$ because $\mathbf{B}_1$ is of the order of several Gauss, while $\mathbf{B}_0 \sim 10^5$ G.

It is not difficult to understand that for the magnetic moment of a sample consisting of a large number of spins $\mathbf{M} = \sum_i \boldsymbol{\mu}_i$ and placed in only a constant field $\mathbf{B}_0$, after the projections of spins onto the z axis and the xy plane are added, the quantity M_z, proportional to the difference between the number n of spins oriented along and against the field, remains constant; simultaneously, we have $M_x = M_y = M_\perp = 0$. This follows from the fact that the phases of precession of individual spins are arbitrary, and therefore, if the number of spins is large, at any instant and for any spin with a certain direction of projection onto the xy plane, there exists another spin with the opposite direction of its projection into the same plane.

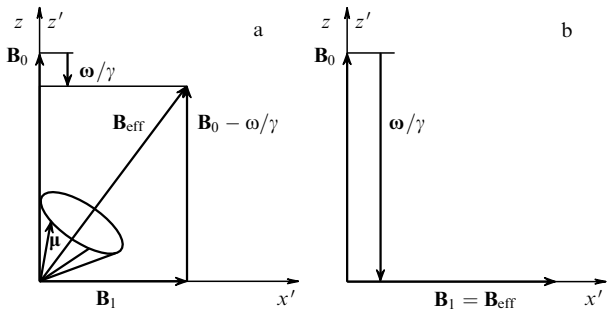

Figure 1. Spin motion in constant and in oscillating magnetic fields: (a) $\boldsymbol{\omega} \neq \gamma\mathbf{B}_0$, (b) $\boldsymbol{\omega} = \gamma\mathbf{B}_0$.

6. Bloch equation

In his initial theory of magnetic resonance, Bloch [1] started with a set of phenomenological equations describing the behavior of the components of the net magnetization vector $\mathbf{M}$. If M is brought out of equilibrium in some fashion, e.g., by turning on a field $\mathbf{B}_1$, then after $\mathbf{B}_1$ is turned off the equilibrium value of $\mathbf{M}$, as Bloch hypothesized, evolves to its equilibrium value in accordance with

$$\frac{\mathrm{d}M_z}{\mathrm{d}t} = \frac{M_0 - M_z}{T_1}\,, \tag{6.1}$$

where M_0 is the equilibrium value of magnetization. But if the equilibrium values of the components M_x and M_y are equal to zero, as established above, Bloch suggested that these components tend to the equilibrium value with a characteristic time T_2 that he called the 'transverse relaxation time.' The corresponding differential expressions are then written as

$$\frac{\mathrm{d}M_x}{\mathrm{d}t} = -\frac{M_x}{T_2}\,,$$
$$\frac{\mathrm{d}M_y}{\mathrm{d}t} = -\frac{M_y}{T_2}\,. \tag{6.2}$$

With the motion of the magnetic moment due to the field $\mathbf{B}_{\mathrm{eff}}$ taken into account in addition to the relaxation terms in Eqns (6.1) and (6.2), we can rewrite the Bloch equation in the rotating frame as

$$\left(\frac{\mathrm{d}\mathbf{M}}{\mathrm{d}t}\right)' = \gamma\,[\boldsymbol{\mu}\mathbf{B}_{\mathrm{eff}}] - \frac{\mathbf{i}M_x' + \mathbf{j}M_y'}{T_2} + \mathbf{k}\,\frac{M_0 - M_z}{T_1}\,. \tag{6.3}$$

Solutions of this equation written for individual components of $\mathbf{M}$ can be found in [1] and in other publications [8, 18]. In the laboratory reference frame, the components M_x' and M_y' rotate around the z axis with the angular frequency ω. Therefore, if the receiver coil is mounted in the xy plane, an emf is generated in it by induction. We note that to characterize absorption, the normalized function of lineshape $g(\omega) = kM_y'$ is often used such that, by definition,

$$\int_{-\infty}^{\infty} g\,(\omega)\,\mathrm{d}\omega = 1\,. \tag{6.4}$$

The Bloch equations and their solutions are mostly valid for NMR lines in liquids. But the concept of relaxation times T_1 and T_2 has universal significance.

7. NMR spectra of liquids and solids. Relation between relaxation times and linewidth

In addition to the external field $\mathbf{B}_0$, nuclei are also exposed to the local magnetic fields $\mathbf{B}_{\text{loc}}$ of their neighbor nuclei and electrons. In diamagnetic materials, the largest are the local fields of neighboring magnetic nuclei; in para- and ferromagnets, the contribution of electrons to $\mathbf{B}_{\text{loc}}$ may be considerably larger. As an estimate, we take the distance between nuclei to be $r \sim 0.1$ nm and assume the magnetic moment of nuclei to be equal to one nuclear magneton; then

$$\mathbf{B}_{\text{loc}} \sim \boldsymbol{\mu} r^{-3} \approx 5 \text{ G},$$

which, in agreement with (2.10), yields the NMR linewidth

$$\Delta\nu \sim 2 \times 10^4 \text{ Hz}.$$

This is an average value that represents the NMR spectrum width in diamagnetic solids within an order of magnitude. In liquids, as a result of fast molecular motions, local fields average down to almost zero, thus leading to very narrow lines. Linewidths measured in many liquids are found to be less than 0.01 Hz (or $\sim 2 \times 10^{-6}$ G). The spin–lattice relaxation time T_1 in liquid and solid samples may vary widely depending on a number of factors (temperature, purity and structure of the sample, presence of paramagnetic impurities), roughly from 10^{-4} to 10^4 s. If the relaxation time is short and the line is narrow, the spectrum width may be determined by the value of T_1. Indeed, a nucleus remains at the given energy level for a time $\Delta t \sim T_1$. The Heisenberg uncertainty relation gives

$$\Delta E \, \Delta t \geqslant h, \tag{7.1}$$

that is, $h\Delta\nu\Delta t \geqslant h$, and the linewidth (in Hz) must be

$$\Delta\nu \geqslant \frac{1}{\Delta t} = \frac{1}{T_1}. \tag{7.2}$$

It is clear that even relaxation times $T_1 \sim 1$ s, not to speak of shorter values, may lead to serious widening of lines in liquids. In pure liquids, the times of transverse or spin–spin relaxation T_2 that characterize the processes of reaching the equilibrium in the spin system in the plane perpendicular to $\mathbf{B}_0$ is often of the same order of magnitude as T_1; in solids however, it is typically much shorter ($\sim 10^{-4}-10^{-6}$ s). Consequently, the linewidth in solids is related to T_2 by the formula

$$\Delta\nu \approx \frac{1}{T_2}. \tag{7.3}$$

Typically, T_2 is calculated using a relation that differs from (7.3) in a numerical coefficient:

$$\Delta\omega = \frac{1}{T_2}, \quad \text{i.e.}, \quad T_2 = \frac{1}{2\pi\Delta\nu}. \tag{7.4}$$

8. Pulse techniques

Hahn [19] was the first to observe the 'spin echo' in 1950 after an RF field pulse was applied to a sample. Advanced pulsed NMR techniques are widely used. As we show below, the pulse and continuous methods of observing NMR are equivalent in principle, but pulse methods often allow extracting information more rapidly or even extracting information that cannot be obtained with continuous NMR. When a sample is exposed to a resonance-frequency field directed along the x' axis in the rotating frame, the effective field $\mathbf{B}_{\text{eff}} = \mathbf{i}B_1$ is applied to the magnetic moment vector $\mathbf{M}$. Therefore, $\mathbf{M}$ rotates in this coordinate system around the x' axis in the $z'y'$ plane with the angular frequency $\boldsymbol{\omega}_1 = \gamma\mathbf{B}_1$ [see (5.7)]. If $\mathbf{B}_1$ is turned on for a short period of time t_{p}, the magnetic moment vector rotates through the angle $\theta = \omega_1 t_{\text{p}} = \gamma B_1 t_{\text{p}}$ (Fig. 2). If the pulse length is chosen to satisfy the condition $\theta = \omega_1 t_{\text{p}} = \pi$, i.e., $t_{\text{p}} = \pi/\gamma B_1$, then after the pulse ends, $\mathbf{M}$ is aligned antiparallel to the applied external field $\mathbf{B}_0$. Such pulses are known as 180-degree pulses, or π-pulses. As a result of a $\pi/2$-pulse oriented along the x' axis, the magnetic moment aligns parallel to y'. In this situation, the magnetic moment is at rest in the rotating frame immediately after $\mathbf{B}_1$ is switched off. Consequently, it precesses in the laboratory frame with the angular frequency $\boldsymbol{\omega}_0 = -\gamma\mathbf{B}_0$, while maintaining an orientation perpendicular to $\mathbf{B}_0$. If the sample is placed in a coil whose axis is in the xy plane, then an emf is induced in it. If all spins were independent and precessed with the same frequency, this emf would remain constant; but as a result of interaction with the environment, different spins have different frequencies. The frequency distribution of spins is in general shaped like a resonance line, for example, the one shown in Fig. 3b. Correspondingly, this produces 'dephasing' of spins in the plane, and the signal reduces to zero. This process can be described by the exponential expression $\mathbf{M}_\perp = \mathbf{M}_0 \exp(-t/T_2)$.

We consider the process of formation of the spin echo. After the arrival of a $\pi/2$-pulse, the net vector $\mathbf{M}$ (which we consider to consist of three spins for illustration purposes) points along the y' axis of the rotating frame. After a time of the order of several T_2, they dephase in the $x'y'$ plane (Fig. 3a, b). We assume that spin *2* precesses at the Larmor frequency $\boldsymbol{\omega}_0 = \gamma\mathbf{B}_0$, while spins *1* and *3* precess at frequencies $\omega_1 > \omega_0 > \omega_3$. If a π-pulse is applied after a time τ, this results in rotating each vector by 180° around the x' axis. Hence, as we see in Fig. 3c, the arrangement of the vectors is reversed: the 'slowest' vector is the one 'in front' and the 'fastest' one is

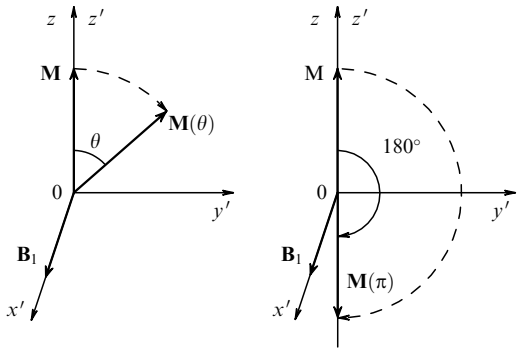

Figure 2. The motion of the magnetic moment $\mathbf{M}$ in a pulsed radio-frequency field.

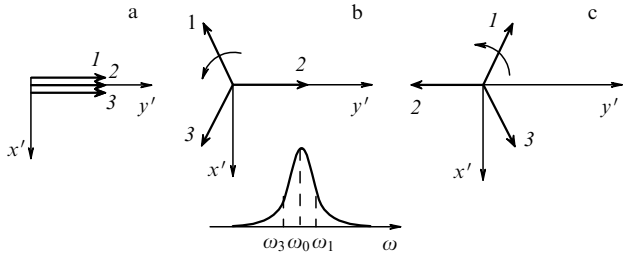

Figure 3. Diagram of the formation of spin echo: (a) after a $\pi/2$-pulse, (b) a short time later, (c) after a π-pulse.

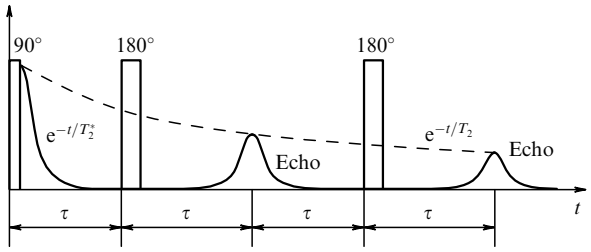

Figure 4. The Carr – Purcell sequence of the formation of spin echo.

'behind.' It is not difficult to understand that the vectors in-phase again after a time 2τ following the beginning of the cycle, producing an echo signal as shown in Fig. 3b.

Carr and Purcell [20] proposed applying π-pulses at the instants $\tau, 3\tau, \ldots, (2n-1)\,\tau$; then echo pulses are generated at the instants $t = 2\tau, 4\tau, \ldots, 2n\tau$. Their amplitude decreases exponentially with the 'true' transverse relaxation time T_2, which can be defined thus (Fig. 4).

We note that because the nuclear magnetization after a 180-degree pulse is antiparallel to $\mathbf{B}_0$, this state can be described, by analogy to (4.7), by using negative spin temperature. We also note that the negative spin temperature corresponds not to a 'colder' but to a 'hotter' state, because additional energy must be transferred to a system of spins at infinite temperature to transform it to a negative-temperature state.

9. Relation between pulse and continuous-wave methods of observation of NMR. Fourier spectroscopy

In 1957, Lowe and Norberg [21] showed that the time of evolution of a spin system of solids after the initial $\pi/2$-pulse in an external magnetic field is related via the Fourier transformation (FT) to the NMR absorption spectrum obtained when the sample is irradiated in a steady-state mode and passes slowly through the resonance. This allowed recording NMR spectra of solids by observing the signal from a spin system after a $\pi/2$-pulse (the so-called free induction decay, or FID), and then performing its Fourier transformation.

If there are no relaxation processes, independent spins precess after the application of a $\pi/2$-pulse with a common frequency, and therefore the time dependence of M can be written as

$$\mathbf{M}_\perp(t) = \mathbf{M}_0 \exp(\mathrm{i}\omega_0 t)\,. \tag{9.1}$$

In actual situations, the sample is characterized by a range of Larmor frequencies; as was demonstrated above, the resonance can then be described by a normalized function of lineshape $g(\omega)$ such that

$$\int_{-\infty}^{\infty} g(\omega)\,\mathrm{d}\omega = 1\,. \tag{9.2}$$

If the $\pi/2$-pulse is made sufficiently short by choosing a high field $\mathbf{B}_1$ such that

$$\gamma B_1 = \omega_1 \gg \Delta\omega\,, \tag{9.3}$$

where $\Delta\omega$ is the width of the resonance curve, then the 'spread' of spins over the duration of the pulse is small and we can assume that all spins are aligned parallel to the y' axis after the pulse. But after the RF field is switched off, the time dependence of $\mathbf{M}_\perp$ in Eqn (9.1) must be replaced with

$$\mathbf{M}_\perp(t) = \mathbf{M}_0 \int_{-\infty}^{\infty} g(\omega)\,\exp(\mathrm{i}\omega t)\,\mathrm{d}\omega = \mathbf{M}_0 G(t)\,, \tag{9.4}$$

where

$$G(t) = \int_{-\infty}^{\infty} g(\omega)\,\exp(\mathrm{i}\omega t)\,\mathrm{d}\omega$$

is the Fourier transform of the lineshape function $g(\omega)$. The function $G(t)$, sometimes referred to as the relaxation function, contains complete characteristics of the decay of the free precession signal $\mathbf{M}_\perp(t)$ after a $\pi/2$-pulse. The inverse Fourier transformation allows finding the lineshape function $g(\omega)$ from the known FID (found from experimental data):

$$\begin{aligned} g(\omega) &= \frac{1}{2\pi M_0}\int_{-\infty}^{\infty} M_\perp(t)\,\exp(-\mathrm{i}\omega t) \\ &= \frac{1}{2\pi}\int_{-\infty}^{\infty} G(t)\exp(-\mathrm{i}\omega t)\,\mathrm{d}t\,. \end{aligned} \tag{9.5}$$

Therefore, expressions (9.4) and (9.5) demonstrate the equivalence of the temporal (pulsed) and spectral approaches: if the function $G(t)$ is known, it is possible to reconstruct the spectrum $g(\omega)$, and vice versa, the FID can be calculated from the known spectrum.

10. Quantum-mechanical description of the main NMR phenomena

So far, with the exception of Section 2, we treated various aspects of NMR using the classical description of this phenomenon. But as was shown, for example, in [16], the results obtained using the classical description are in fact identical to those obtained by applying rigorous quantum mechanical methods.

In the simplest case of noninteracting spins, it is not difficult to find eigenvalues of the quantum mechanical Hamiltonian that determines the energy spectrum levels of a system. In actual situations, the Hamiltonian may contain a group of other terms in addition to the terms responsible for the coupling of spins to the magnetic field (constant or alternating), i.e., for the Zeeman interaction. The main terms for spin-1/2 nuclei are the Hamiltonian H_d of the direct dipole – dipole magnetic interaction, which can in turn

be split into the Hamiltonians H_{dII} of the homonuclear and H_{dIS} of the heteronuclear interactions.

Nuclei with spin greater than 1/2 have a quadrupole moment that is coupled to the electric field gradient at the point of localization of these nuclei. The energy operator of this interaction, H_{q}, may contribute substantially to the total Hamiltonian. The electrons surrounding the nucleus shield the external magnetic field, causing a shift in the Larmor frequency (the so-called chemical shift) because the electron shielding depends on the location of the resonating nuclei in the molecule. The corresponding Hamiltonian is $H_\sigma = \gamma\hbar\sum_j \sigma_j \mathbf{I}_{zj}$, where σ_j is the shielding constant. Nuclear magnetic moments can interact both directly and indirectly by polarizing the electron shells of the atom and transferring this polarization to neighboring nuclei. This indirect spin–spin interaction, also known as the scalar interaction, is described by a term of the type $H_j = \sum_{ij} \mathbf{J}_{ij}\,\mathbf{I}_i\,\mathbf{I}_j$, where $\mathbf{J}_{ij}$ is the spin–spin coupling constant.

In principle, other types of couplings can also be taken into account, e.g., the spin–lattice coupling of nuclear spins, the coupling of nuclear spins to unpaired electrons in paramagnetic matter, the coupling to conduction electrons in metals (the Knight shift), and the spin–orbit coupling [18].

The main Hamiltonian of a real system placed in a magnetic field (constant or alternating) can therefore be rewritten as

$$H = H_{\mathrm{Z}} + H_{\mathrm{d}} + H_{\mathrm{q}} + H_{\mathrm{ot}}\,, \tag{10.1}$$

where H_{ot} are the other terms of the interaction.

Hamiltonian (10.1) can also be split into two terms characterizing the interaction of spins with internal and external fields (the Zeeman interaction):

$$H = H_{\mathrm{Z}} + H_{\mathrm{int}}, \tag{10.2}$$

where H_{int} are all the other terms of Hamiltonian (10.1) except H_{Z}.

The above types of internal interactions exist in all fundamental states of matter: liquid, solid, and gas, but the characteristics and intensity of these interactions depend essentially on the state of matter [22]. For example, all terms of the Hamiltonian H_{int} of a solid can be written in tensor form because all the interactions listed above are essentially anisotropic. In liquids, the interactions H_{d} and H_{q} are averaged to zero owing to fast motion of molecules, and only scalar quantities remain instead of the tensor characteristics of the chemical shift and indirect spin–spin interaction. Therefore, the information that can be obtained using the NMR in solids is much richer in principle than in liquids. However, the NMR spectroscopy in liquids had progressed much faster until recently because of the visual clarity and accessibility of averaged values of chemical shifts of various nuclei and of constants of the spin–spin interaction between them. Enormous arrays of the corresponding accumulated experimental data obtained by NMR spectroscopy of liquids have benefited and continue to bring huge benefits to various fields of chemistry, biology, and medical sciences. In the last 20–25 years, however, considerable progress has been achieved in 'simplifying' the spectrum of solids and in extracting very rich and valuable information. Modern multipulse NMR techniques for solids allow efficiently eliminating certain types of interaction from spectra, thereby improving the observation of other interactions that carry valuable information on the systems under study. For instance, the efficient suppression of the homonuclear dipolar interaction with protons allowed the observation of the indirect dipole–dipole interaction between carbon ^{13}C nuclei, which is usually hidden behind a stronger direct dipole–dipole interaction with protons [23–27].

In principle, once the Hamiltonian of the system is written with the actual interactions involving spins taken into account, a quantum mechanical calculation of the NMR spectrum reduces to calculating the spectrum of eigenvalues of the Hamiltonian (of the system of energy levels) and of the probabilities of transitions between these levels, which determine the intensities of individual lines in the spectrum. Although the principle used to find solutions of these problems is quite well known — its description can be found in any textbook on quantum mechanics (see, e.g., [17]) — its practical implementation may encounter certain difficulties in a number of cases. Specific methods of spectrum calculations suitable for concrete situation of NMR in solids and liquids are given in a number of textbooks [16, 28], in the excellent monograph by Ernst, Bodenhausen, and Wokaun [29], and in some other monographs [5, 6, 8].

The method of description using the density matrix (outlined below) has become widely used in research and development of new multipulse sequences. In addition to classical analytic approaches to the description of NMR experiments, numerical techniques for the calculation of spectra are now very popular. Efficient numerical techniques for specific NMR measurements in solids are described in more detail in a number of recent publications [30–36].

11. The density matrix and its application to NMR spectrum calculations

The NMR signal is typically recorded using a coil whose axis is perpendicular to $\mathbf{B}_0$ and lies in the xy plane [in the laboratory frame (LF)]. The emf induced in the coil equals the rate of change of the total magnetic flux $\mathbf{\Phi}$ through the coil. Because $\mathbf{\Phi}$ is proportional to the nuclear magnetization $\mathbf{M}_x$, which varies as $\mathbf{M}_x = \mathbf{M}_{x0}\sin\omega t$, the induced emf (with phase ignored) is

$$\varepsilon = -\frac{\mathrm{d}\Phi}{\mathrm{d}t} = k'\,\frac{\mathrm{d}M_x}{\mathrm{d}t} = kM_x\,, \tag{11.1}$$

where k and k' are constants.

The nuclear magnetization $\mathbf{M}_x$ is the mean value $\langle\mathbf{M}_x\rangle$ of the operator of macroscopic magnetic moment. The mean value of a physical quantity f that corresponds to the operator $\mathbf{f}$ is known [16, 17] to be given by

$$\langle\mathbf{f}\rangle = \int \psi^*\,\mathbf{f}\,\psi\,\mathrm{d}q = \sum_{m,n} c_m^* c_n \int \psi_m^* f \psi_n\,\mathrm{d}q$$

$$= \sum_{m,n} c_m^* c_n f_{mn}(t)\,, \tag{11.2}$$

where

$$\psi = \sum c_n\,\psi_n \tag{11.3}$$

is a decomposition of an arbitrary wave function with respect to wave functions of steady states. The matrix element of the

corresponding transition from state m to state n is

$$\int \psi_m^* f \psi_n \, \mathrm{d}q = \left(m \,|f|\, n\right) = f_{mn}(t) \,. \tag{11.4}$$

As we see from (11.2), to calculate the mean value of some quantity, we only need to know the product $c_m^* c_n$ and not the quantities c_m and c_n separately. We now rewrite (11.2) as

$$\langle f \rangle = \sum_{m,n} \rho_{mn} f_{mn}(t) \,, \tag{11.5}$$

where ρ_{mn} are matrix elements of the statistical operator ρ of the density matrix.

Using the density matrix formalism is especially convenient for calculations of various effects produced by a number of factors on the spin system as it evolves with time. We write the basic relations for the density matrix and its matrix elements [16, 37]. The evolution of ρ with time is described by the von Neumann equation

$$\mathrm{i}\hbar \frac{\partial \rho}{\partial t} = [H, \rho] = H\rho - \rho H \,, \tag{11.6}$$

where $[H, \rho]$ is the commutator of the density matrix and the Hamiltonian of the system. The mean value of any physical variable represented by an operator $\mathbf{f}$ is given by

$$\langle \mathbf{f} \rangle = \mathrm{Tr}\,(\rho \mathbf{f}) \,,$$

where Tr is the trace of a matrix, equal to the sum of its diagonal elements. The solution of Eqn (11.6) is written as

$$\rho(t) = U(t)\, \rho(0)\, U^{-1}(t) \,, \tag{11.7}$$

where $\rho(0)$ is the density matrix at $t = 0$ and $U = \exp\left[(-\mathrm{i}/\hbar)\, Ht\right]$. For time-dependent matrix elements, it was shown in [16, 37] that

$$\rho_{mn}(t) = \exp\left[\frac{\mathrm{i}}{\hbar}\,(E_m - E_n)\, t\right] \rho_{mn}(0) \,. \tag{11.8}$$

We now write an explicit expression for the density matrix operator (see [16], p. 180):

$$\rho = \frac{1}{Z} \exp\left(-\frac{H}{kT}\right) = \frac{\exp\left(-H/kT\right)}{\mathrm{Sp}\left[\exp\left(-H/kT\right)\right]} \,, \tag{11.9}$$

where

$$Z = \sum_n \exp\left(-\frac{E_n}{kT}\right) \tag{11.10}$$

is the partition function.

It is now possible to calculate the signal generated in matter by the applied pulse. Let a pulse of duration t_p and frequency $\boldsymbol{\omega}_0 = \gamma \mathbf{B}_0$ act on a spin system that is in dipole–dipole interaction with the Hamiltonian H_d. Then the Hamiltonian of the problem is

$$H = H_\mathrm{Z} + H_\mathrm{d} + \mathbf{H}_1(t) \,, \tag{11.11}$$

where $H_1(t) = \gamma \mathbf{B}_1 \hbar \mathbf{I}_x \cos \omega t$. In principle, while the RF field pulse lasts, calculating $\rho(t)$ requires using a time-dependent Hamiltonian. For example, if we take a $\pi/2$-pulse with a small $t_\mathrm{p} = (\pi/2)\, \gamma B_1$ (large B_1), then in the total Hamiltonian we can drop the terms that do not commute with H_Z or $H_1(t)$. This is equivalent to assuming that as a result of a short duration of the pulse, its spectrum is much broader than the spread of Larmor frequencies caused by the dipole–dipole interaction. Therefore, during the pulse, we have

$$\rho(t) = \exp\left(-\frac{\mathrm{i}}{\hbar} H_1 t\right) \rho(0) \exp\left(\frac{\mathrm{i}}{\hbar} H_1 t\right) , \tag{11.12}$$

where H_1 is given by (11.11).

The calculation of $\rho(t)$ with a time-dependent Hamiltonian may in general be a fairly complicated problem; but in our case, it is readily shown that [8]

$$\rho(t) = I_z \cos\alpha - I_y \sin\alpha \,, \tag{11.13}$$

where α is the angle of rotation of magnetization caused by the pulse: $\alpha = \gamma \mathbf{B}_1 t_\mathrm{p}$. If $\alpha = \pi/2$, we have $\rho(t) = -I_y$ after the pulse ends, i.e., the action of the pulse amounts to a rotation of magnetization into the xy plane.

After the end of the pulse, the Hamiltonian becomes time-independent; this greatly simplifies the calculation of the density-matrix evolution. For instance, if a system that was initially in equilibrium with a density matrix $\rho(0)$ is subjected to two pulses with an interval τ between them, then after the second pulse ends, we have

$$\rho(t) = U_\mathrm{IV} U_\mathrm{III} U_\mathrm{II} U_\mathrm{I} \rho(0)\, U_\mathrm{I}^{-1} U_\mathrm{II}^{-1} U_\mathrm{III}^{-1} U_\mathrm{IV}^{-1} \,, \tag{11.14}$$

where the subscripts I and III of unitary operators [see (11.7)] refer to the period within a pulse, II to the interval between pulses, and IV to the time after the second pulse ends.

Calculating the mean magnetization in the xy plane as

$$\left\langle M(x,y) \right\rangle = \mathrm{Tr}\left[\rho(t), M_{x,y}\right] , \tag{11.15}$$

we find the signal in the receiving coil

$$\varepsilon = S(t) = k \left\langle M(x,y) \right\rangle = k\, \mathrm{Tr}\left[\rho(t), M_{x,y}\right] . \tag{11.16}$$

We note that a detailed description of the application of the density matrix formalism to calculations of the NMR spectrum under chemical exchange was given in the monograph by Kaplan and Fraenkel [38].

12. Molecular mobility and NMR spectra

The application of nuclear magnetic resonance to the study of internal mobility in crystals has opened a number of new possibilities for studying the properties of solids. Current theoretical understanding indicates that there is a direct relation between intracrystalline mobility (vibrations, diffusion, internal rotation or reorientation of atoms, molecules, or molecular groups) and the fundamental aspects of solid-state physics. On the other hand, many practically important characteristics of solids — dielectric permittivity, plasticity, specific heat, phase transitions, etc. — are also closely related to internal mobility. A number of experimental methods are available to extract information on molecular mobility. NMR techniques undoubtedly occupy an important place among them. Among their advantages, we can point to the relative ease of obtaining results in a wide temperature range, the possibility (in principle) of extracting information about all

the above-mentioned types of internal mobility, and the high sensitivity to very slow motions (several Hz and even fractions of a Hz). It is not accidental, therefore, that the emergence of the NMR method has provided new impetus to the experimental study and to rethinking solid-state physics in the presence of internal motion.

It became clear soon after NMR was discovered that the width and shape of the NMR spectrum are related most closely to the mobility of nuclei. In the general case, with sufficiently fast nuclear motions, averaging the local fields results in narrowing and reshaping of NMR spectra.

The foundations of the theory of the effect of mobility of nuclei on the NMR spectrum were laid out in the fundamental work by Bloembergen, Purcell, and Pound (BPP) [39]. Molecules or groups of atoms in solids at sufficiently low temperatures occupy one of the configurations corresponding to a minimum of their potential energy, and perform only fairly small-amplitude oscillations in the potential well. As temperature increases, the oscillation energy increases, resulting in an increased probability of a molecule going over the potential barrier and transferring to a different equilibrium configuration via rotation through a certain angle (reorientational motion) or via translation (diffusional motion). In most cases, this process can be described by a single correlation time τ_C characterizing the average lifetime of a molecule in this state. The number of molecules whose energy suffices for overcoming the potential barrier V_0 increases with the temperature; typically, τ_C changes exponentially:

$$\tau_C = \tau_0 \exp\left(\frac{V_0}{kT}\right), \tag{12.1}$$

where τ_0 is a constant; it is also possible to introduce the correlational frequency of motion that satisfies the condition

$$2\pi\nu_C\tau_C = 1\,. \tag{12.2}$$

Then

$$\nu_C = \nu_0 \exp\left(-\frac{V_0}{kT}\right), \tag{12.3}$$

where

$$2\pi\nu_0\tau_0 = 1\,. \tag{12.4}$$

As shown in [39], for sufficiently high speeds of molecular motion,

$$\nu_C \geqslant \Delta\nu \;(\tau_C \leqslant T_2)\,, \tag{12.5}$$

where $\Delta\nu = \gamma\Delta B_0/2\pi$ is the line width for a rigid lattice and spins 'feel' the time-averaged local field. In general, this mean field is smaller than the local field for a rigid lattice and therefore rapid motions satisfying condition (12.5) make the NMR spectrum narrower.

13. Methods of obtaining high-resolution NMR spectra in solids

13.1 'Magic'-angle spinning

The first high-resolution spectra in solids were obtained in solid samples through averaging the dipole–dipole interaction by Andrew [40] and Lowe [41], who used a macroscopic sample spinning at a 'magic' angle (MAS) [18, 42].

If a system of spins experiences interactions that are weak compared to the Zeeman interaction, then its spectrum falls in the vicinity of the Larmor frequency $\boldsymbol{\omega}_0 = \gamma\mathbf{B}_0$. The structure of such spectra depends on the Hamiltonian H of the system and the spectrum width can be evaluated by expressing its 'value' denoted by $\|H\|$ in frequency units. If H varies with a period $\tau = 1/\nu$, then the structure of the spectrum also changes. If the condition of fast motion similar to (12.5) also holds ($\tau < T_2$ or $\nu > \Delta\nu$), the spectrum can be described in terms of a time-dependent mean Hamiltonian $\langle H\rangle$. In the general case, $\|\langle H\rangle\| < \|H\|$, which allows speaking of an efficient narrowing of the spectrum and of a possible 'switching off' of some components of the Hamiltonian and of separating its other components of interest.

The dipole–dipole nuclear interaction carries useful information on the location of nuclear spins in crystals, which is the foundation for application of NMR techniques to structure research. But the same interaction is harmful in some cases because it masks weaker effects (e.g., chemical shift and scalar spin–spin interaction) owing to its relatively high strength. In view of this, work has been going on for a relatively long time on developing various NMR methods for line narrowing in order to achieve 'high resolution' in solids. Among such methods, we mention rapid sample spinning at a magic angle [41, 43, 44], the experimental methods of Lee and Goldburg [45], and pulsed techniques suggested by Waugh and Mansfield for line narrowing in solids [46–50]. The main feature of all these methods is the periodic variation in time of the internuclear dipole–dipole interaction such that it averages to zero over each period.

Specific methods developed by Waugh's group allow averaging the component H_d of the Hamiltonian H that corresponds to the dipole–dipole interactions, and singling out the much weaker components representing the chemical shift, the spin–spin interaction, etc. to be studied.

The NMR spectrum of a system of spins manifesting the dipole–dipole nuclear interaction is determined by the secular, i.e., time-averaged component of the Hamiltonian H_d, which can be written for spins of the same type as [8, 51]

$$H_d^0 = \frac{\gamma^2\hbar^2}{2}\sum_{j>k}\mathbf{r}_{jk}^{-3}(3\cos^2\theta_{jk} - 1)\,(\mathbf{I}_j\mathbf{I}_k - 3I_{zj}I_{zk})\,, \tag{13.1}$$

where $\mathbf{r}_{jk}$ is the vector connecting two nuclei (spins) j and k, θ_{jk} is the angle between $\mathbf{r}_{jk}$ and $\mathbf{B}_0$, and $\mathbf{I}_j$, $\mathbf{I}_k$, I_{zj}, and I_{zk} are the operators of spins and of their z-projections.

The NMR spectrum defined by Hamiltonian (13.1) for a two-spin system (the nuclei in a solid form isolated pairs, e.g., protons of water molecules in crystal hydrates) was first calculated by Pake [52]. The spectrum of such a system is written as

$$\mathbf{B}_{0\text{res}} = \mathbf{B}_0 \pm \mathbf{b}_{\text{loc}} = \mathbf{B}_0 \pm \frac{3}{2}\,\boldsymbol{\mu}\,r_{12}^{-3}\,(3\cos^2\theta_{12} - 1)\,, \tag{13.2}$$

where $\mathbf{B}_0$ is the resonance value of the field for isolated nuclei, the subscripts 1 and 2 label the nuclei in a pair, and θ_{12} is the angle between the direction of the magnetic field $\mathbf{B}_0$ and the internuclear vector $\mathbf{r}_{12}$.

As we see from formula (13.2), the spectrum of a two-spin system is a doublet whose components are symmetric with respect to $\mathbf{B}_0$, and the distance between the components is

$$\Delta\mathbf{B} = \frac{3}{2}\,\boldsymbol{\mu}\,r_{12}^{-3}\,(3\cos^2\theta_{12} - 1)\,. \tag{13.3}$$

If $\theta_{12} = 0$, the maximum distance between these components is

$$\Delta\mathbf{B} = 3\boldsymbol{\mu} r_{12}^{-3} . \tag{13.3a}$$

This gives approximately 21 G for water molecules in crystal hydrates.

In experiments with a sample spinning at the magic angle θ_{jk} that corresponds to the condition $3\cos^2\theta_{jk} - 1 = 0$, dipole interactions average to zero, as we see from (13.1).

It can be shown that rapid spinning of the sample (MAS) affects many other types of anisotropic interactions in solids in this manner, reducing the direct dipole interaction (homo- and heteronuclear), the shielding anisotropy (chemical shift), the Knight shift in metals, the indirect spin – spin interaction, and the electric quadrupole interaction.

Therefore, MAS often leads to the generation of high-resolution spectra in solids, similar to spectra in liquids, which greatly enhances their information content and makes them especially valuable for studying polycrystalline and amorphous samples [42].

13.2 Multipulse transformation of spectra

By using pulses to control the orientation of spins, it is possible to average the expression in the second pair of parentheses in (13.1) [46 – 49]. One of the first sequences for pulse-induced line narrowing, the so-called four-pulse cycle WHH-4 (WHH is formed of the initial letters of the names Waugh, Haeberlen, and Huber), is shown in Fig. 5. Here, P_x, P_{-x}, P_{-y}, and P_y are $\pi/2$-pulses for which the phase shift of the RF field equals 0, 180, 270, and 90 degrees. It is clear from the description of the behavior of a pulse-irradiated system of spins (see Section 5) that after the P_x pulse (whose RF field is directed along the x' axis of the rotating frame), all spins are aligned in the direction of the y' axis of this system. The next pulse P_{-x}, whose RF field is antiparallel to the x' axis, returns magnetization to the direction of the z axis (which is parallel to the external field $\mathbf{B}_0$). Then the pulse P_{-y} aligns the spins parallel to the x' axis, and the pulse P_y again returns them to the orientation along z. This cycle of length t_C is repeated periodically.

We consider the behavior of a system of spins within one period. The Hamiltonian averaged over the time t_C, with the intervals between pulses as indicated in Fig. 5, has the form

$$\langle H_d^0 \rangle = \frac{1}{3}\left(H_{dx}^0 + H_{dy}^0 + H_{dz}^0\right). \tag{13.4}$$

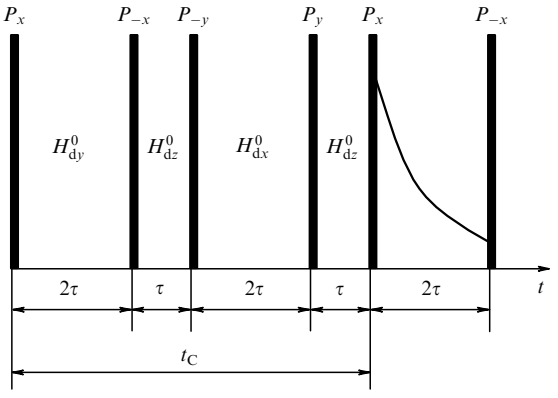

Figure 5. The four-pulse WHH-4 sequence for line narrowing in solids.

This implies that the averaged Hamiltonian $\langle H_d^0 \rangle$ vanishes over the duration of one cycle. As shown in [53], the chemical shift survives but is reduced by a factor of $\sqrt{3}$.

Furthermore, high power and high homogeneity of the RF field are required to run this cycle. To eliminate this and other shortcomings of the WHH-4 sequence, dozens of versions of different sequences that generate high-resolution spectra of solids have been proposed [10, 50, 51, 54 – 60]. In this way, the pulse narrowing techniques produced a large amount of data on the chemical shift in the spectra of solids (see papers [61, 62] and the monograph by Mering and Haeberlen [22]).

The pulse sequence WHH-4 was a precursor of a number of novel techniques [63]. One of the problems encountered with the WHH-4 sequence was that while averaging the Hamiltonian

$$\langle H^0 \rangle = \int_{t=0}^{t_C} H(t)\,\mathrm{d}t \tag{13.5}$$

over the period t_C to zero, this sequence was unable to average the first-order correction to it given by the formula

$$\langle H^1 \rangle = \int_{t_1=0}^{t_C}\int_{t_2=0}^{t_1} \left[H(t_2), H(t_1)\right] \mathrm{d}t_2\,\mathrm{d}t_1 . \tag{13.6}$$

It was shown that this problem can be solved by using pulse sequences in which the basic four-pulse WHH-4 block is repeated with a common phase shift [22, 53, 59, 60, 64, 65]. More intricate pulse sequences allow averaging higher-order correction terms to zero as well.

Another method of averaging the homonuclear dipole interaction was suggested by Lee and Goldburg [45]. In this case, suppression is achieved by using off-resonance irradiation of the sample with a powerful RF field. To achieve total suppression, the frequency shift from the resonance and the intensity of the RF field must obey the relation

$$\frac{\omega_1}{\Delta\omega_0} = \tan\theta_M = \sqrt{2} . \tag{13.7}$$

Under these conditions, the magnetization vector precesses in the rotating frame (chosen relative to the off-resonance irradiation) around the axis tilted at the magic angle $\theta_M = 54.7^\circ$ to the external magnetic field. In the same way as in the case of the WHH-4 sequence, the chemical shift reduces by a factor of $\sqrt{3}$.

As in the case of WHH-4, the simple Lee – Goldburg method again cannot provide averaging to zero of the first correction term to the averaged dipole Hamiltonian. To overcome this difficulty, a modified Lee – Goldburg experiment with frequency switching was suggested [66, 67]. In this technique, continuous irradiation is replaced with a sequence of short bursts. Each burst consists of two pulses at frequencies that are shifted from the NMR resonance frequency by $+\Delta\omega_0$ and $-\Delta\omega_0$ (i.e., lie on both sides of the central frequency of the spectrum). The maximum efficiency of the homonuclear decoupling is achieved when the length τ_p of each pulse is selected such that the magnetization vector completes a total revolution around the tilted effective field:

$$\tau_p = \frac{2\pi}{\omega_{eff}} , \tag{13.8}$$

where

$$\omega_{\text{eff}} = \sqrt{\omega_1^2 + \Delta\omega^2} \tag{13.9}$$

is the effective value of the precession frequency under off-resonance irradiation.

A new version of this experiment was recently suggested, in which the off-resonance irradiation is replaced with irradiation at the NMR resonance frequency with a linearly scanned phase [68 – 70].

The third type of the pulse-sequence technique for suppressing the effects of homonuclear interaction is based on a pulse sequence of 'magic echo' (see Section 25). Rhim et al. showed [71] that a specially designed pulse sequence may reverse the time evolution of a coherent spin state induced by the homonuclear dipole – dipole interaction. The effect of the dipole interaction can therefore be suppressed; this opens a way to recording high-resolution spectra. The method as originally suggested involved a large number of pulses and was highly sensitive to the intensity and homogeneity of the RF field. It was later expanded and improved in [72 – 75]. These methods are sometimes referred to in the literature as techniques based on the 'magic sandwich' echo. An advantage of this type of pulse narrowing (it includes the sequences TREV-8 [72] and MSHOT-3 [74, 75]) is that the averaged Hamiltonian of the chemical shift causes rotation of the magnetization vector around the direction of the external magnetic field. In the case of the WHH-4 sequence and the Lee – Goldburg experiment, the rotation occurs only around the tilted axis, which results in undesirable artifacts on the NMR spectrum. A substantial reduction of the chemical shift by a factor of 0.3 – 0.4 is also one of the shortcomings of the TREV-8 and MSHOT-3 techniques.

Experimental factors such as the inhomogeneity of the RF field in the bulk of the sample, and phase and amplitude errors in RF pulses may considerably reduce the efficiency of suppression [22, 76, 77]. Methods based on direct computerized optimization of the pulse sequence help to overcome these complications, albeit incompletely. The pulse phases in the continuous experimental run were used as an optimization parameter, and either the computer model [78] or the experimental NMR spectrum directly [79] was used as the response function.

We note that pulse narrowing is often used in combination with magic-angle spinning. If the MAS frequency is much lower than the RF field frequency, then MAS does not reduce the efficiency of pulse narrowing [80]. At the same time, MAS may be adequate for suppressing all other sources of line broadening in solid-state NMR, such as the chemical shift anisotropy. The method of combined pulse narrowing and MAS (Combined Rotation and MultiPulse Spectroscopy, CRAMPS) [81] can produce NMR spectra that carry information only on isotropic interactions, such as the chemical shift and indirect dipole – dipole interaction, by suppressing the anisotropic component of the interaction. We must also mention pulse techniques in which the sequences are synchronized with MAS in order to suppress a number of interactions [82].

14. Rare-spin NMR

Another very important breakthrough that opened new avenues in NMR research in solids came with techniques developed by Waugh and Pines at the beginning of the 1970s [83] aimed at generating high-resolution spectra of rare isotopes; the success allowed studying NMR in solids of virtually all elements of the periodic table. Multiple experiments carried out using these techniques are described in adequate detail in monographs [18, 22, 84] and papers [11, 13, 14].

We consider a system with spins of two types, **I** and **S**, in which, owing to the chemical or isotopic dilution, the number of spins **I** is much larger than the number of spins **S**. This situation is encountered, for instance, in organic compounds, where ^{1}H plays the role of the predominant population of spins and ^{13}C are rare spins.

Obviously, if we wish to observe the NMR of rare spins, at least two problems have to be faced: insufficient sensitivity because the number of spins **S** in the sample is very small, and the fact that resonance lines of rare spins are usually greatly broadened due to the dipole – dipole interaction with the predominant spins **I**, which typically have a high gyromagnetic ratio. This dipole broadening can be eliminated if the predominant spins are strongly irradiated at the resonance frequency $\boldsymbol{\omega}_{\mathbf{I}} = \gamma_{\mathbf{I}}\mathbf{B}_0$. In principle, the sensitivity problem is solved by using the idea of Hartmann and Hahn [85] on the possibility of bringing spins **I** and **S** in 'thermal contact' in the rotating frame if the condition

$$\gamma_{\mathbf{I}} B_{1\mathbf{I}} = \gamma_{\mathbf{S}} B_{1\mathbf{S}} \tag{14.1}$$

is satisfied.

Quite a few methods are available now to practically implement the principles outlined above for the observation of the NMR of rare spins. They are discussed in detail in an excellent review by Pines, Gibby, and Waugh [83]. Without going into the details, we here consider only one of these methods, sufficiently simple and convenient, suggested by these three authors in [86]. Most of the studies of the NMR of rare spins in solids were carried out using this technique. When a sample is placed in a magnetic field $\mathbf{B}_0$, after a time of the order of $T_{1\mathbf{I}}$, the spin system acquires the nuclear magnetization

$$M_{\mathbf{I}}^{(0)} = \frac{C_{\mathbf{I}} B_0}{T_{\mathrm{L}}}\,, \tag{14.2}$$

where C_{I} is the Curie constant and T_{L} is the lattice temperature. Then a sequence of pulses is sent that aligns the spins **I** in the rotating frame along the direction of $\mathbf{B}_{1\mathbf{I}}$. If $T_{1\mathbf{I}}$ is sufficiently high, the magnetization $M_{\mathbf{I}}^{(0)}$ cannot change significantly during the first $\pi/2$-pulse and we can write the Curie law in the rotating frame as

$$M_{\mathbf{I}}^{(0)} = \frac{C_{\mathbf{I}} B_{1\mathbf{I}}}{T_\gamma}\,, \tag{14.3}$$

where T_γ is the temperature in the rotating frame. From (14.2) and (14.3), we now find

$$\frac{T_\gamma}{T_{\mathrm{L}}} = \frac{B_1}{B_0}\,. \tag{14.4}$$

Equation (14.4) shows that the system of spins **I** in the rotating frame is considerably cooled, because $B_1 \ll B_0$. Then the system of spins **S** is put in thermal contact with the system **I** by sending an RF field at the resonance frequency of spins **S**, i.e., $\boldsymbol{\omega}_{\mathrm{S}} = \gamma_{\mathbf{S}}\mathbf{B}_0$, with the amplitude $\mathbf{B}_{1\mathbf{S}}$ selected in accordance

with Hartmann – Hahn condition (14.1). If this condition is satisfied, intense flip-flopping of spins **I** and **S** occurs; the total energy of the system remains unchanged and the system rapidly reaches thermodynamic equilibrium. As a result of this contact with the cold system of spins **I**, the system **S** is cooled, which means that a certain degree of ordering arises in it as the magnetization along $\mathbf{B}_{1S}$. At the same time, the system **I** becomes somewhat warmer (its magnetization decreases), but this heating is insignificant because **S** spins are rare and the heat capacity of this system is much lower than that of the system of spins **I**. The field $\mathbf{B}_{1S}$ is then turned off and the free induction decay (FID) of spins **S** is observed while the spins **I** are still exposed to one of the pulse sequences for suppression of the heteronuclear dipole – dipole interaction. In this process, the FID of rare spins accumulates and then the Fourier transformation yields high-resolution high-intensity spectra of rare spins. To increase the NMR resolution of the spectra of rare nuclei and to suppress anisotropic interactions such as the anisotropy of chemical shift, the above method of cross-polarization is combined with magic angle spinning [87].

15. 2D Fourier spectroscopy

The next important stage in the progress of high-resolution NMR in solids arrived when two-dimensional (2D) Fourier spectroscopy was introduced. Jeener was the first to introduce the idea of this method in 1971 [88], but its practical implementation to solid objects started only in 1976 with independent publications by three groups: Lippmaa [89], Waugh [90, 91], and Vega and Vaughan [92].

2D Fourier spectroscopy often leads to radically enhanced resolving power and improved segregation of various interactions in NMR spectra.

In the specific case of solids, when a sample simultaneously contains, e.g., ^{13}C and ^{1}H nuclei, the chemical shift on carbon nuclei may be masked by the ^{13}C – ^{1}H dipole – dipole interaction such that the carbon spectrum cannot be resolved in principle with the ordinary one-dimensional representation. The 2D spectroscopy allows separating the chemical shift and dipole interaction and plotting them on individual axes. A conclusive example of such separation is shown in Fig. 6, mostly taken from [93] but modified for the purposes of this paper. The upper part of this figure plots an ordinary one-dimensional spectrum (in fact, a projection of the two-dimensional spectrum onto the ν_2 axis). We see that the dipole – dipole interaction between protons and carbon in the methylene group CH_2 manifests itself in the one-dimensional spectrum only as a broadening of the corresponding line. At the same time, the heteronuclear dipole interaction ^{13}C – ^{1}H with two hydrogen atoms that are nonequivalent at a given orientation of the single crystal are clearly pronounced in the two-dimensional spectrum along the ν_1 axis. As the figure clearly shows, ^{13}C nuclei of other groups, which contain no nearby protons, are represented by single lines, as in the one-dimensional spectrum, whose chemical shift is determined by their position on the ν_2 axis.

This example clearly illustrates the advantages of the 2D Fourier spectroscopy, even though it by no means exhausts the potential of specific modifications of the method that allows separating various interactions in solids. All versions of using the 2D spectroscopy can, however, be arranged into some sort of common framework [94]. The schematic diagram of the experiment aimed at producing a two-

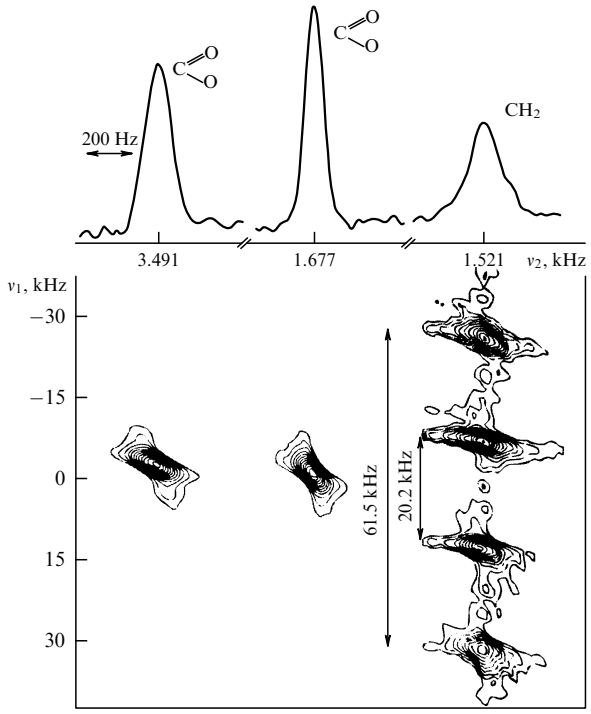

Figure 6. A two-dimensional NMR spectrum of ^{13}C in a CH_2COONH_4COOH single crystal.

dimensional spectrum is shown in Fig. 7a. The entire experiment can be divided into four phases: 1— preparation, 2 — evolution, 3 — mixing, 4 — recording; phases 1, 2, and 4 are 'mandatory' for obtaining two-dimensional spectra; the mixing period is used only in some special experiments. During the preparation phase, the system is transformed from thermodynamic equilibrium to a nonequilibrium state. This is done most often, although not always, by using a $\pi/2$-pulse. Then the system is allowed to evolve under the action of the Hamiltonian H_1, which can reflect all internal interactions in the sample but can also be somehow 'transformed,' e.g., by 'switching off' the homonuclear dipole – dipole interaction using a multipulse sequence (see Section 13). The signal of the spin system, which is described in phase 4 by a Hamiltonian H_2 that differs from H_1, is recorded over a time t_2. If the nuclear magnetization is recorded many times for different lengths of the evolution period t_1, it is possible to obtain a two-dimensional FID $M(t_1, t_2)$ that yields the two-dimensional spectrum $S(\omega_1, \omega_2)$ after a two-dimensional Fourier transformation. To obtain this spectrum, the two-dimensional Fourier transformation is calculated in accordance with the expression

$$S(\omega_1, \omega_2) = \int_0^\infty \mathrm{d}t_1 \exp(-\mathrm{i}\omega_1 t_1) \times \int_0^\infty \mathrm{d}t_2 \exp(-\mathrm{i}\omega_2 t_2)\, M(t_1, t_2)\,.$$

In 1978, Ernst et al. [95] proposed a 'block diagram' developed for designing various versions of the two-dimensional Fourier spectroscopy based on program blocks and corresponding to different phases of the general diagram (see Fig. 7).

As an illustration, we examine generating a 2D in the WISE experiment [96]. This experiment creates a link between

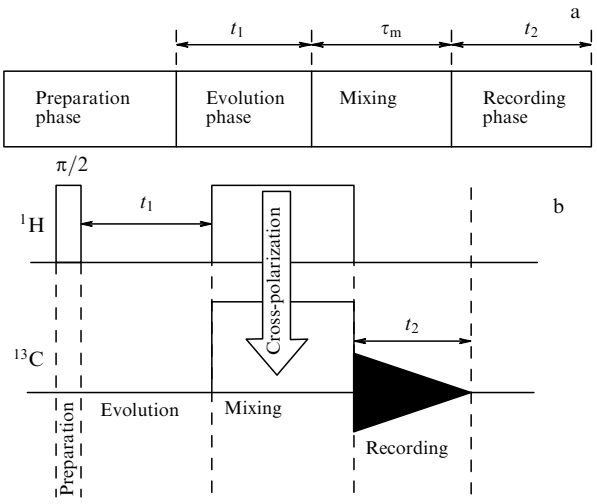

Figure 7. (a) General diagram of recording 2D NMR spectra; (b) diagram of a 2D WISE experiment.

spectra of rare nuclei (e.g., ^{13}C) recorded in the first dimension and the spectrum of protons recorded in the second dimension of the 2D spectrum. The WISE technique is based on cross-polarization of rare spins (Fig. 7b). To obtain the correlation spectrum, an evolution phase t_1 is inserted between the initial $\pi/2$-pulse (which is essentially the preparation phase) and the spin-lock phase. During this entire phase, the proton magnetization precesses freely in the xy plane of the rotating frame governed by the Hamiltonian of the proton chemical shift. Therefore, for the proton spin **I** with chemical shift ω, the spin-lock affects the component proportional to $\cos \omega t_1$. If the cross-polarization period is sufficiently short, each signal in the rare-spin spectrum is produced by the nearest protons and each individual signal in the spectra of rare spins is also proportional to $\cos \omega_i t_1$, where ω_i is the chemical shift of the nearest-neighbor protons. Therefore, a sequence of one-dimensional spectra with different durations of the evolution phase t_1 additionally contains information on chemical shifts of the nearest-neighbor protons responsible for the process of cross-polarization.

However, this information is inadequate for using the 2D Fourier spectroscopy, because it does not allow separation of contributions from protons with a chemical shift equal in magnitude but opposite in sign. A similar problem in the one-dimensional NMR spectroscopy is solved using quadrature detection, when one of the receiver channels records a signal proportional to the cosine component, while the second, phase-shifted by 90°, records the sine component of the signal. It does not appear possible to obtain both components of the signal simultaneously in the 2D NMR spectroscopy. Several methods are known for overcoming this problem. For instance, in the States method [97], not one but two spectra are recorded for each evolution time t_1. For the second spectrum, the initial $\pi/2$-pulse is phase-shifted by 90° and shapes a signal proportional to $\sin \omega_i t_1$. As the NMR signal is being processed, these two components are 'mixed' and form a complex signal required for the Fourier transformation in the second dimension. In addition to the States method, the method of time-proportional phase increment (TPPI), the mixed States–TPPI method, or the echo–antiecho method [97] are also used.

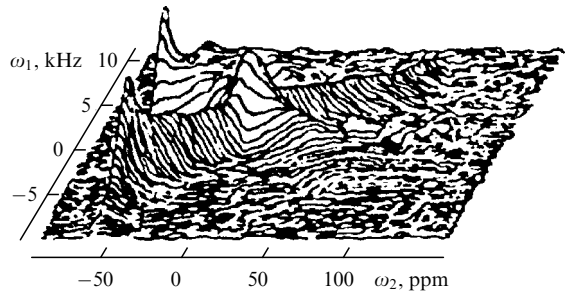

Figure 8. 2D spectrum of solid polycrystalline benzene.

The potentials of the 2D spectroscopy in studying polycrystalline samples and problems that arise when this method is used were discussed in [98]. In particular, that paper gave examples of separation of chemical shift tensors and the dipole–dipole interaction and of determination of their parameters in solids. Figure 8 shows the NMR spectrum of polycrystalline benzene at the frequency 25 MHz and the temperature $T = 148$ K. The experiment was designed such that one of the axes (ω_2) reproduced only the chemical shift and the other the chemical shift in combination with the dipole–dipole interaction reduced by a factor of $1/\sqrt{3}$. Other examples of the application of two-dimensional NMR spectroscopy are discussed in [18, 29, 84, 99] and in papers [11, 13, 14].

16. Multiquantum NMR spectroscopy

It is well-know that NMR spectroscopy normally uses transitions between neighboring spin levels in a magnetic field; transitions are controlled by selection rules $\Delta m = \pm 1$. Both in optics and in NMR and EPR in a low field, m is frequently not a 'good quantum number' and consequently transitions with $\Delta m = \pm 2$ become possible because of state mixing. But this is still a single-quantum transition, not to be confused with truly two- and multiquantum processes involving actual absorption of n quanta by the spin system in transitions with $\Delta m = n$.

Here, we do not go into detail about double-quantum spectroscopy and three-level systems with the spin $I = 1$, e.g. deuterons or nitrogen ^{14}N, which allow generation of spectra in solids in the presence of strong quadrupole broadening; indeed, these aspects were discussed quite thoroughly in papers [29, 100–102] and monographs [18, 29, 84].

We consider a multilevel system that is formed in a group of strongly interacting spins $I = 1/2$, e.g., protons in benzene C_6H_6 ($N = 6$) in a strong magnetic field B_0. If we take only the intramolecular interaction into account, then the z-component of the total spin can take one of the $N+1$ values corresponding to their magnetic quantum numbers $M = \Sigma m_i$ in the range $-N/2 \leqslant M \leqslant +N/2$ (Fig. 9). For any given M, the levels of noninteracting spins are degenerate. The interaction within a group of spins, which in a strong field is much weaker than the Zeeman interaction, removes the degeneration (see Fig. 9), but M remains a good quantum number, i.e., levels with unequal M are separated sufficiently well from each other. Such systems allow multiquantum transitions, e.g., the ($n = N$)-quantum transition between highest and lowest levels with $\Delta M = N$, which yields a single line at the frequency $\omega = \omega_0 + n\Delta\omega - \Sigma\sigma_j \omega_0$ [103, 104]. This expression shows that the resonance of an n-quantum transition is shifted relative to ω_0 by $n\Delta\omega$ and by the sum of

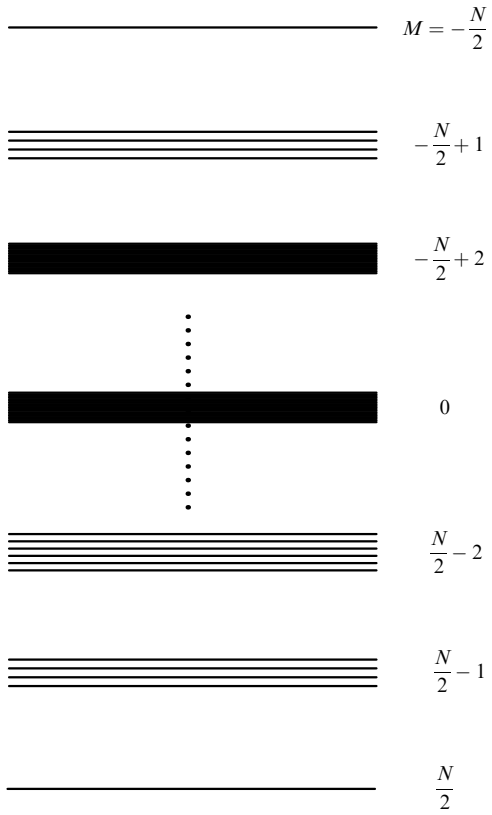

Figure 9. Energy level diagram of a group of strongly interacting spins.

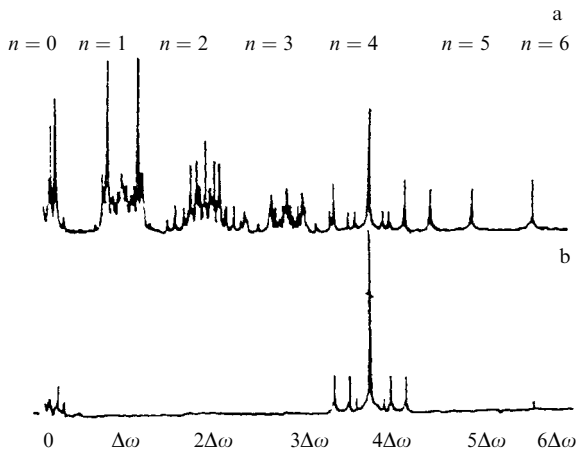

Figure 10. (a) Multiquantum spectrum of benzene in a liquid crystal and (b) selectively singled-out four-quantum spectrum.

the chemical shifts $\sigma_j \omega_0$. Because the dipole – dipole interaction is bilinear, it is unchanged under simultaneous flipping of all spins and does not affect the transition frequency; that is, the N-quantum NMR spectroscopy is high-resolution spectroscopy in solids. Pines et al. [103 – 106] noticed that the dipole – dipole interaction also affects other transitions and that $(N-1)$- and $(N-2)$-quantum transitions can be used for studying structure and mobility in solids. Figure 10a illustrates the n-quantum spectrum ($n = 0, 1, 2, 3, 4, 5, 6$) of benzene in a liquid crystal [105]. This system has N levels with $M = \pm(N/2-1)$ and $N(N-1)/2$ levels with $M = \pm(N/2-2)$. With the dipole interaction taken into account, the $(N-1)$-quantum spectrum should have 6 pairs of lines $(-N/2+1) \leftrightarrow N/2$; $(N/2-1) \leftrightarrow -N/2$ (see Fig. 9), i.e., 6 pairs of lines in the case of benzene ($N-1=5$). But all six protons in benzene are equivalent and therefore, as we see from Fig. 10a, we only have a single pair of lines. Therefore, the number of pairs of lines in the $(N-1)$-quantum spectrum equals the number of nonequivalent spin configurations in the system. The number of lines in benzene for an $(N-2)$-quantum spectrum must be $N(N-1) = 30$ (see [105]). However, owing to the symmetry of the molecule, we only see three lines (Fig. 10a) corresponding to the pairwise dipole – dipole interaction between protons in ortho-, meta-, and paraconfigurations.

There exist many different ways of exciting 'coherent states' of all levels in a multilevel system that allow observation of multiquantum transitions. The simplest method of generating such coherent states is to expose the system to two $\pi/2$-pulses separated by a time interval τ [84, 106, 107].

But this coherent precession cannot be observed directly [107]. To record multiquantum transitions, a third 90-degree pulse is sent after an evolution time t_1 following the second $\pi/2$-pulse, and then magnetization is taken into account after a time t_2. To obtain the total spectrum, it is necessary to vary t_1 at constant τ and t_2 and to vary the set of values of τ and t_2.

The problem of how to single out a specific transition from all possible n-quantum transitions for a given n was discussed in [108, 109]. The intensity of signals from high-n transitions decreases considerably if the suggestions proposed in these papers are used for observation. Pines et al. [103 – 106] discussed and experimentally demonstrated how a given n-quantum transition can be selectively singled out without losing high intensity. Figure 10b in [105] shows that the selectively separated 4-quantum transition in this particular case even exceeds the corresponding single-quantum transition in intensity.

Multiquantum spectroscopy with $n > 2$ was used at the beginning mostly to interpret complex spectra in liquids, to analyze 'isolated' spin groups linked to aligned molecules in liquid crystals, etc. When solids were studied, only the double-quantum spectroscopy was involved [18, 84]. Later, higher-order transitions came into use for such purposes [110 – 112].

Pines et al. [112] turned their attention to the dynamics of spin systems in solids and reported interesting results on temporal correlation between processes that determine the FID through ordinary single-quantum transitions and intensification of higher-order multispin coherence. They were able to use multiquantum spectra of various proton-containing solids to experimentally trace the temporal evolution of multispin correlations induced by dipole interaction. Using deuterated 1.8-dimethylnaphtalene (except for methyl groups) as an example, they succeeded in demonstrating that multiquantum spectroscopy of isolated spin clusters allows evaluating the number of spins per group. Pines and co-workers concluded [112] that applications of their technique may prove very fruitful in various fields of physics and chemistry and especially for studying isolated molecules in solid matrices and molecules adsorbed on surfaces of solids.

The method of multiquantum NMR spectroscopy in combination with 'magic angle' spinning (MQMAS) became widespread for generating high-resolution NMR spectra of quadrupole nuclei with half-integral spin [12, 113, 114].

We have given only a brief exposition of the principles of the method without any detailed description of the theory or of numerous experimental techniques for exciting multi-

quantum coherence. These aspects are discussed thoroughly in an excellent monograph [29], which devotes a chapter and a half to this subject.

17. Molecular mobility in solids. Mobility in crystals and NMR spectra

Traditionally, the study of internal mobility in solids using NMR has received much attention. In what follows, we discuss certain possible approaches to such studies.

17.1 Reorientations around different axes

Gutowsky and Pake [115] considered reorientational motion of a system of two nuclei around an axis (Fig. 11). In this figure, $\mathbf{r}_{jk}$ is the vector connecting nuclei j and k (this vector is at an angle θ_{jk} to the direction of the magnetic field $\mathbf{B}_0$); $0N$ is the axis of reorientation that forms an angle θ' with $\mathbf{B}_0$ and an angle γ_{jk} with $\mathbf{r}_{jk}$. These authors succeeded in showing that when the $0N$ axis is a threefold or higher-order axis, reorientation at a sufficiently high frequency is equivalent to free rotation of the vector $\mathbf{r}_{jk}$ around this axis. It was also discovered that as in the case of rigid lattices, the spectrum consists of two lines, but the distance between them is given by the formula

$$\Delta B = \frac{3}{2}\,\mu r_{jk}^{-3}\,(3\cos^2\theta' - 1)\,(3\cos^2\gamma_{jk} - 1)\,. \qquad (17.1)$$

If $\gamma_{jk} = \pi/2$, i.e., if the reorientation axis is perpendicular to the internuclear vector, we have

$$\Delta B = \frac{3}{2}\,\mu r_{jk}^{-3}\,(3\cos^2\theta' - 1)\,, \qquad (17.2)$$

and the spectrum manifests two lines separated by the maximum distance equal to half the distance for a rigid system [see (13.3a)]. If θ' is the magic angle, i.e., $3\cos^2\theta' - 1 = 0$, then the dipole–dipole interaction, as many another interactions, does not manifest itself in the spectrum, which in this case is a single spectral line.

The effect of reorientation around a twofold axis on the NMR spectrum of a solid was discussed in [116]. In a

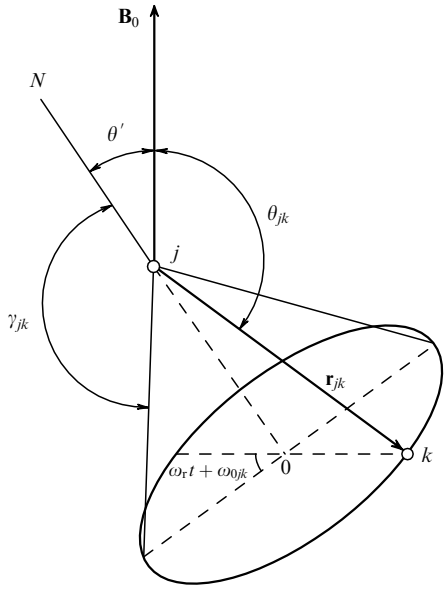

Figure 11. Diagram of reorientation of nuclei around a fixed axis.

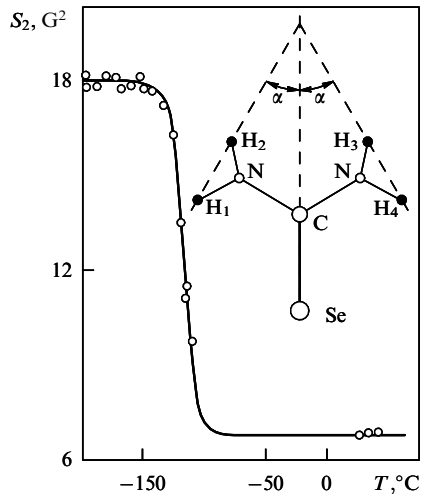

Figure 12. Temperature dependence of the second moment for selenourea.

selenourea molecule $SeC(NH_2)_2$, whose atoms all lie in one plane, there is a twofold axis (Fig. 12) passing through the atoms of SeC. This axis lies at angles of about 30 degrees to the interproton vectors H_1-H_2 and H_3-H_4. For clarity, we consider the case where the magnetic field $\mathbf{B}_0$ points at the initial instant along the vector H_1-H_2. For this pair, therefore, the local fields are

$$b_{1,2} = \pm\frac{3}{2}\,\mu r^{-3}\,(3\cos^2 0^\circ - 1) = \pm 3\mu r^{-3}\,; \qquad (17.3)$$

for the pair H_3-H_4, they are

$$b_{3,4} = \pm\frac{3}{2}\,\mu r^{-3}\,(3\cos^2 60^\circ - 1) \approx \mp\frac{3}{8}\,\mu r^{-3}\,. \qquad (17.4)$$

At a sufficiently low temperature, when the lattice is rigid, i.e., the condition $v_c \ll \Delta v$ holds, the spectrum is formed by two lines — two Pake doublets spaced by the distance

$$\Delta B_1 = 2b_{1,2} = 6\mu r^{-3} \quad \text{and} \quad \Delta B_2 = 2b_{3,4} = \frac{3}{4}\,\mu r^{-3} \qquad (17.5)$$

within each doublet.

As temperature increases, reorientation frequency v_c for the molecule $SeC(NH_2)_2$ rotating through the 180° angle around the twofold axis in accordance with (12.5) increases. If it becomes larger than the line width for the rigid lattice ($\Delta v \sim 10^4$ Hz), we neglect the time of transition ($t \sim 10^{-12}$ s) and can express the local field at the proton as the mean value of the two equilibrium configurations of the molecule:

$$\langle b\rangle = \frac{b_{1,2} + b_{3,4}}{2} = \left(\pm 3\mu r^{-3} \mp \frac{3}{8}\,\mu r^{-3}\right)\frac{1}{2} = \pm\frac{21}{16}\,\mu r^{-3}\,. \qquad (17.6)$$

In this case, therefore, the spectrum consists of a single doublet with the distance

$$\Delta B = 2\langle b\rangle = \frac{21}{8}\,\mu r^{-3} \qquad (17.7)$$

between its components.

This example clearly demonstrates that reorientation around a twofold axis may result in a substantial narrowing and modification of the NMR spectrum.

The ratio of the second moments S_2 in a polycrystalline specimen in this case is (see Section 18) S_2^{p} for reorientable molecules and S_2^{r} for a rigid lattice [116]

$$\frac{S_2^{\mathrm{p}}}{S_2^{\mathrm{r}}} = \frac{3\cos^2\alpha - 1}{4}\,. \tag{17.8}$$

Figure 12 plots the temperature dependence of the second moment for selenourea. Using this and applying formula (17.8), we can find that $\alpha \approx 30^\circ$.

17.2 NMR spectra and the diffusion of atoms and molecules in crystals

In accordance with the BPP theory, the averaging of local magnetic fields in the process of *atomic* diffusion through a crystal lattice leads to abrupt narrowing of the NMR line if the diffusion rate is sufficiently high [8, 39]. This behavior of the spectrum under diffusion has been reported for a number of metals, metal hydrides, and nonmetallic solids.

An aspect of considerable interest is the quantitative description of the effect that diffusion of *molecules* has on the NMR spectrum in solids; as an example, we here consider the diffusion of water molecules in crystals. It is well known that the spectra of crystallization water molecules in a rigid lattice are doublets with the maximum distance between components about 21 G (see Section 13.1). However, spectra of some water-molecule-containing crystals emerge as a single doublet, with the distance between its components also depending on the orientation of the crystal in the magnetic field, while the angular dependence of splitting often cannot be reflected in a formula similar to (13.3a). Furthermore, $\Delta B_{\max}$ never reaches the value 21 G but falls in the range $\Delta B_{\max} \approx 1-10$ G, being different for different crystals. Such spectra were observed, in particular, by Yano [117] and Ducros [118]. Such spectra can be explained on the basis of the model of diffusion of water molecules through the crystal lattice [119]. Moreover, the experimental study of NMR spectra provides unique information on molecular diffusion in crystals. We consider a crystal with a regular structure incorporating H_2O molecules. In such a crystal, we can expect, by analogy with Schottky atomic vacancies, the presence of molecular vacancies, i.e., lattice sites not occupied by water molecules. The equilibrium concentration n of vacancies is given by the relation

$$n = \frac{N_{\mathrm{B}}}{N} \approx \exp\left(-\frac{\Delta E_{\mathrm{B}}}{kT}\right), \tag{17.9}$$

where N_{B} is the number of vacancies in the crystal, N is the total number of molecules, and ΔE_{B} is the energy of vacancy formation. For an H_2O molecule, we have $\Delta E_{\mathrm{B}} \sim 20$ kJ mole^{-1}. At room temperature, this gives $n \sim 10^{-4}$. The mean vacancy lifetime at a given lattice site, calculated using standard formulas [120], is $\sim 10^{-8}$ s (for $T = 300$ K). Taking (17.9) into account, this shows that on average each water molecule at room temperature changes its localization 10^4 times per second. In accordance with the BPP theory [39], this results in dynamic narrowing of the NMR spectrum. Clearly, a change in ΔE_{B} can shift this temperature in one direction or another.

A molecule in each of the consecutively occupied lattice sites in the process of diffusion must be oriented in a way characteristic of the given site such that hydrogen bonds of maximum strength can be formed. In other words, during diffusion, a molecule passes through a discrete set of positions and orientations found on lattice sites. If the time of transition from one lattice site to another is much shorter than the lifetime of the molecule at each site (which is the normal situation), then averaging the local field simply reduces to the mean value $\langle b\rangle$ for the ensemble of molecules, in accordance with their positions and orientations of the p – p vectors in the rigid lattice of the crystal. It was shown in [119, 121, 122] that because the dipole interaction depends on the distance between the nuclei as $1/r^3$, the shape of the spectrum is mostly determined by the intramolecular interaction between protons in the water molecule, while the intermolecular interaction mostly affects the width of spectrum components.

In the general case, the motion of a water molecule taking part in diffusion can be modeled as a combination of parallel translations between fixed lattice sites and rotations from one fixed orientation at one site to another fixed orientation at another site. Parallel translations of p – p vectors do not change the local field b [see (13.2)] because the angles remain unchanged; hence, only rotations must be taken into account. If the p – p vector of water molecules assumes i structurally allowed positions in the process of diffusion and each of these positions is characterized by a relative weight p_i, with $\sum_i p_i = 1$, then the mean value of the intramolecular component of the local field is

$$\langle b^{\mathrm{intra}}\rangle = \sum_i p_i b_i = \pm\frac{3}{2}\,\mu r^{-3}\sum_i p_i\,(3\cos^2\theta_{jk}^i - 1)\,. \tag{17.10}$$

Therefore, calculating an NMR spectrum in the case of diffusion reduces to calculating the effect of the combination of possible rotations of the molecule on $\langle b\rangle$.

At a sufficiently low temperature, such that diffusion is too slow for local fields to be averaged in time, each of the allowed configurations of the water molecule produces their doublet in accordance with (13.2) and their relative intensities and angular dependence can be easily established experimentally.

Molecular diffusion, as well as experimental results for different crystals, is discussed in more detail in [119, 122] and in the book by Gabuda and Lundin [121]. Convenient calculation formulas based on a tensor representation of the dipole interaction are given in [123].

18. The method of moments

If magnetic nuclei are randomly distributed through a solid, there is no point in calculating the spectrum because the fine details cannot be resolved in the experiment anyway due to the broadening of individual components caused by the interaction with nuclei. It is still possible, however, to extract some useful structural information without resorting to an analysis of lineshape. Van Vleck was able to show [124] that quantitative characteristics are available that relate the experimentally observed NMR spectra of solids to the arrangement of nuclei in the sample. Moments of spectra are such characteristics. If the normalized lineshape is described, as before, by the function $g(b)$, then the nth moment of the spectrum, denoted here by S_n, is given by

$$S_n = \int_{-\infty}^{\infty} b^n g(b)\,\mathrm{d}b\,, \tag{18.1}$$

where b is the local field [see (9.2) and (13.2)]. Because the NMR spectrum broadened by the dipole–dipole nuclear interaction is symmetric with respect to the field $\mathbf{B}_{0\text{res}}$, all odd moments of the spectrum vanish ($b = 0$).

Van Vleck [124] derived expressions that relate the second and fourth moments of the NMR spectrum to the mutual arrangement of nuclei in a crystal. Structural applications of NMR techniques mostly use the formula for the second moment; expressions for higher-order moments are used rather infrequently [125–128]. The Van Vleck formula for S_2 can be written as [124, 129]

$$S_2 = \frac{3}{4} I(I+1)\gamma^2\hbar^2 \frac{1}{m}\sum_{j=1}^{m}\sum_{k} r_{jk}^{-6}(3\cos^2\theta_{jk} - 1)^2 + \frac{1}{3}\hbar^2 \frac{1}{m}\sum_{j=1}^{m}\sum_{f} I_f(I_f+1)\gamma_f^2 \sum_{k_f}(3\cos^2\theta_{jk_f} - 1)^2 r_{jk_f}^{-6}. \quad (18.2)$$

The indices j and k in this expression refer to nuclei at which the resonance is observed, the index f labels other species of nuclei, and the index k_f labels nuclei within each species; m is the number of structurally nonequivalent nuclei in one unit cell of the crystal; I, I_f, γ, and γ_f are the spins and gyromagnetic ratios of the corresponding nuclei; and the quantities r and θ have the same meaning as in formula (13.2).

The second moment for a polycrystalline sample is equal to the mean value of the second moments of isotropically distributed crystals; hence, averaging (18.2) over the angles θ_{jk} and θ_{jk_f} yields

$$S_2 = \frac{3}{5} I(I+1)\gamma^2\hbar^2 \frac{1}{m}\sum_{j=1}^{m}\sum_{k} r_{jk}^{-6} + \frac{4}{15}\frac{1}{m}\hbar^2\sum_{j=1}^{m}\sum_{f} I_f(I_f+1)\gamma_f^2\sum_{k_f} r_{jk_f}^{-6}. \quad (18.3)$$

Having recorded the NMR spectrum of a polycrystalline sample and calculated its second moment using (18.1), we gain the possibility of comparing it with the quantity S_2 found from (18.3) for a specific configuration of nuclei. Of course, there is an infinite number of ways nuclei can be distributed in agreement with their experimentally observed second moment. Nevertheless, the method of second moments is quite useful even in this modification as a simple method that tests the correctness of specific models, e.g., those postulated or defined on the basis of diffraction data. Indeed, if the second moment calculated using formula (18.3) differs greatly from the experimentally found value, this is unequivocal evidence of an incorrect initial model.

A much greater volume of structural information is generated by using the angular dependences of second moments. McCall and Hamming [129] constructed a compact mathematical theory of this case by introducing a coordinate system with x, y, z axes anchored rigidly in the crystal lattice.

The problem of finding the number N of independent parameters by analyzing the orientational dependence of the second moment of the NMR spectrum of a single crystal in a magnetic field was solved in [127, 130] using the tensor representation. The table above lists the results obtained and also the numbers of independent parameters for the orientational dependence of the fourth moment $S_4(\theta, \varphi)$. We see, for example, that $N(S_2) = 15$ for the triclinic system; therefore, placing the origin of coordinates at the point of localization of one of the nuclei, we can find the mutual arrangement of six nuclei in a unit cell of the crystal (three coordinates for each of the remaining five nuclei).

Table. The number of linearly independent parameters N describing the functions $S_2(\theta, \varphi)$ and $S_4(\theta, \varphi)$.

Crystallographic system	Laue group	$N(S_2)$	$N(S_4)$
Triclinic	1	15	45
Monoclinic	$2/m$	9	25
Rhombic	mmm	6	15
Trigonal	$\bar{3}$	5	15
	$\bar{3}m$	4	10
Tetragonal	$4/m$	5	13
	$4/mmm$	4	9
Hexagonal	$6/m$	3	9
	$6/mmm$	3	7
Cubic	$m3$	2	5
	$m3m$	2	4

The solution of the problem of calculating the coordinates of nuclei with maximum accuracy and minimum effort was obtained in [127, 130, 131] using the theory of optimal experimental design [132–134]. The experimental results in [127] on finding the coordinates of light nuclei in crystals show that the achieved localization accuracy is comparable with that provided by neutron diffraction. This allows treating the NMR as an independent physical method for determining the mutual arrangement of light nuclei in crystals. In a number of cases, NMR techniques allow extracting information that cannot be obtained using diffraction-based techniques. For instance, X-ray diffraction yields the center-of-mass coordinates of the electron shells of atoms, which in the case of light atoms may be very different from the coordinates of the nuclei. Oscillations of nuclei in crystals manifest themselves differently by NMR and neutron diffraction, which, on the one hand, sometimes leads to appreciable differences between coordinates calculated using the two methods, but on the other hand offers a unique chance of studying these oscillations.

19. Suppression of the heteronuclear dipolar interaction with protons in solids (proton decoupling)

Rare nuclei, such as ^{13}C, strongly interact in organic solids with more widespread nuclei, typically protons. This interaction results in substantial broadening of magnetic resonance lines. To narrow NMR lines and improve resolution of NMR spectra, methods of suppression of the heteronuclear dipole interaction are used. Such methods constitute a direct analogy to the heteronuclear decoupling of NMR in liquids, but while the main interaction resulting in NMR line broadening in liquids is the indirect dipole–dipole interaction, the role of the main heteronuclear interaction in solids is played by the direct dipole–dipole interaction.

As in the case of liquids, the simplest method of decoupling from protons is the continuous irradiation of samples at the NMR frequency of protons. However, the direct heteronuclear dipolar interaction is stronger by several orders of magnitude than the indirect interaction in the same compound (tens kHz and hundreds of Hertz, respectively). As a result, complete suppression requires application of a much more powerful RF field. Typically, the suppressing radiation

should be on for the entire time of detection of the signal, that is, of the order of several milliseconds. Application of such long and powerful pulses is one of the main technical problems of NMR in solids, because excessively prolonged decoupling may result in overheating and failure of NMR probes.

In principle, continuous decoupling is based on stimulating fast transitions of irradiated spins (usually protons) from one level to another. Consequently, the heteronuclear dipole–dipole interaction continually changes sign, which produces averaging to zero [135].

To increase the efficiency of suppression of the heteronuclear dipole interaction, a number of multipulse techniques have been suggested, as happened earlier in the case of liquids. But the methods that work well for the NMR of liquids are unsuitable for the NMR of solids, due to differences in the strength of the heteronuclear interaction, interference between homo- and heteronuclear coupling, and interference with spectral components when a sample is spun at a magic angle.

Multipulse techniques suggested in recent years [136–139] have led to substantial improvements in the resolution of spectra of rare nuclei.

A theoretical foundation of the methods of suppressing the dipolar interaction with protons under MAS conditions can be provided using the mean Hamiltonian theory [139–142] or the Floquet theory [143]. We note that a description of multipulse methods of decoupling from protons is a fairly complicated task because it requires an analysis of a system of protons interacting via the homonuclear dipole interaction.

We have to admit that, roughly speaking, any such multipulse sequence not only suppresses the heteronuclear dipole interaction but also affects the term of the Hamiltonian responsible for the homonuclear interproton flip-flop interaction. This phenomenon improves the resolution of spectra of rare nuclei and is now known as 'self-decoupling.'

We note in conclusion that the method proposed by Stejskal, Schaefer and Waugh [87], which uses cross-polarization to improve sensitivity and MAS techniques for suppressing the interaction with protons so as to improve resolution, has become essentially the main technique for obtaining high-resolution spectra of rare nuclei in solids.

20. Methods of reconstruction of anisotropic interactions under MAS conditions

Spinning (rotation) at the magic angle effectively suppresses anisotropic interactions in solids. This improves the resolution of NMR spectra and consequently increases the volume and quality of information learnt about the systems under study. However, anisotropic interactions carry very important information on various characteristics of sample. To reliably identify these interactions, it is preferable, on the one hand, to insure that the quality of the NMR spectrum obtained with MAS does not change considerably, but on the other hand, that other types of anisotropic interactions appreciably affect the spectra. Furthermore, the repeated introduction of anisotropic interactions ought to be done very selectively so as to separate effects of different types of interactions. For instance, it is extremely desirable to run an experiment that would permit observation of the dipole–dipole interaction between different groups of atoms with resolved peaks in MAS NMR spectra, thereby eliminating the effect, e.g., of anisotropy of the chemical shift or of the quadrupole interaction. We have to recognize that considerable progress has been achieved in this area in recent years.

One of the most popular methods of reconstructing the heteronuclear dipolar interaction is now the method of rotational-echo double resonance (REDOR) [144]. It is used for measuring heteronuclear interaction in the case of isolated pairs of spins.

The heteronuclear Hamiltonian for isolated pairs of spins I–S in a MAS experiment can be written as [22]

$$H_{\mathrm{IS}}(t) = -\frac{1}{2}\, b_{\mathrm{IS}} \{ \sin^2\beta \cos 2(\gamma + \omega_r t) - \sqrt{2} \sin 2\beta \cos(\gamma + \omega_r t) \}\, 2I_z S_z \,,$$

where

$$b_{\mathrm{IS}} = -\left(\frac{\mu_0}{4\pi}\right) \frac{\gamma_{\mathrm{I}} \gamma_{\mathrm{S}} \hbar}{r_{\mathrm{IS}}^3}$$

is the dipole–dipole coupling constant. The Euler angles β and γ describe the position of the internuclear vector I–S in the system of coordinates coupled to a rotor spinning at the magic angle. If the rotation proceeds at high angular velocity, the quantity in parentheses vanishes and $\langle H \rangle = 0$.

But if the π-pulse is applied for one of the spins at an interval equal to half the length of the rotation cycle (see Fig. 13), then the spin term $I_z S_z$ reverses its sign. Therefore, the signal of the spin I at the instant of detection depends on the value of the Hamiltonian H_{IS}. The undesirable contribution of the chemical-shift Hamiltonian is refocused by using the Hahn spin echo.

It is questionable whether REDOR can be used successfully with systems of more than two spins. However, modifications of the method have recently been proposed that yield valuable information on the dipole–dipole interaction for such systems, too [145–148].

In addition to REDOR, a number of other similar techniques are available. For instance, cross-polarization under MAS conditions also leads to reconstruction of the dipole–dipole interaction and may be used for measuring its intensity [149]. Methods are also known that allow selective measurement of the homonuclear dipole interaction [150–157], the anisotropy of the chemical shift [158–160], and so forth. Levitt et al. suggested a fairly interesting class of sequences in which the difference in behavior of Hamiltonians of various interactions relative to symmetry operations is used [141, 161, 162]. This approach generated whole families of pulse sequences both for selective suppression and for the reconstruction of interactions in solids under MAS conditions.

21. Methods of computer simulation of NMR spectra

Computerized calculations of NMR spectra are based on the principles described above. For computer simulation, all spin operators must be converted to matrix format. As a rule, these matrices are written in terms of the system of eigenfunctions of the operator I_z or, as is also known, the Zeeman system, in which the quantization axis points in the direction of the magnetic field $\mathbf{B}_0$.

Using the matrix form of spin operators allows constructing the Hamiltonian and the density matrix of the spin system required to solve von Neumann equation (11.6).

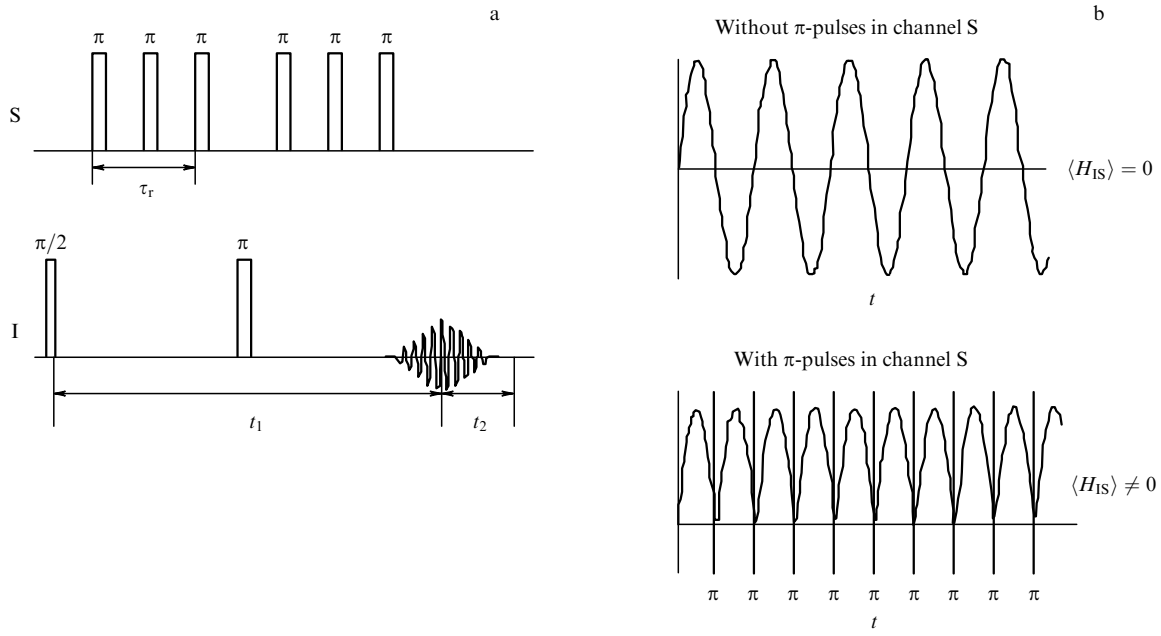

Figure 13. REDOR experiment: (a) pulse sequence; (b) illustration of the principle of the method.

Most interactions in solids are anisotropic and therefore the Hamiltonian of the spin system must be converted to tensor format. As a rule, the Hamiltonian of each interaction λ is transformed for these purposes using irreducible spherical tensors:

$$H_\lambda = \sum_l \sum_{m=-l}^{l} (-1)^m R^\lambda_{l,-m} T_{l,m} ,$$

where $R^\lambda_{l,-m}$ is the spatial component of the interaction λ and $T_{l,m}$ is the spin operator. One advantage of this representation lies in the simplicity of describing the rotations of both the spin and the spatial components of the Hamiltonian.

The Hamiltonian of the system in most of contemporary NMR experiments is time-dependent. For instance, MAS continuously modifies the spatial component of the Hamiltonian for anisotropic types of interaction. On the other hand, the application of multipulse sequences implies that during the time the RF field acts on the sample, the Hamiltonian of the interaction with the RF field must be added to the internal Hamiltonian [see Eqns (11.12) and (11.14)]. In a computer simulation of time-dependent Hamiltonians, the entire time of the experiment is divided into short intervals during which the Hamiltonian is assumed to be constant. To find the density matrix at an instant t, Eqn (11.14) is used. The free precession signal can also be found from Eqn (11.16). In the case of quadrature detection, the magnetization operator is proportional to the raising operator:

$$M_{x,y} \propto F_+ = F_x + iF_y ,$$

where $F_q = \sum_i I_{iq}$ and i labels spins in a spin system.

Computer simulation for powder samples requires multiple reruns for different orientations of the spin system relative to the magnetic field. The resulting signal of free induction is the sum of the FID obtained for different orientations.

Numerical simulation of NMR spectra, especially for spectra of large systems or for complicated pulse sequences, severely taxes computer resources. Correspondingly, large effort has been devoted to optimizing algorithms of such computations. For instance, the number of orientations of a spin system can be reduced in the computation of the spectra of powders by using special algorithms [163 – 167]. When an NMR spectrum of a powder sample is computed under MAS conditions, averaging crystal orientations over one of the Euler angles can be combined with computations for different time instants when the sample spins are at the magic angle [168]. A block diagonal [32] or sparse [36] structure of a matrix involved in the computations can be used for speeding up the computation of exponential operators in Eqn (11.7). If the geometry of a model spin system has translational symmetry, then the Hamiltonian and the density matrix can be transformed to a block diagonal form [169]. This opens possibilities for simulating systems with a fairly large number of spins (15 to 16) using conventional desktop computers. Such model systems are capable of qualitatively reproducing NMR specifics of typical nuclei, such as ^{1}H [170, 171], which is regarded as one of the most complicated tasks in the NMR theory.

Specific implementations of the above-described algorithms make up part of a number of programs and computer packages [30, 31, 36, 172, 173].

22. Phase transitions in solids

NMR is long known as a method that works successfully in studying phase transitions in crystals. First of all, because the width of the spectrum (and its second moment) depends on the mutual arrangement of nuclei, shifting of nuclei due to a phase transition may cause the spectrum to change. Such a change stemming from a shift in proton positions has been observed, for instance, in the response to ferroelectric phase transitions [174 – 176]. Another possibility involves observation of the resonance with nuclei having quadrupole moments. Because the tensor of the electric field gradient (EFG) at a nucleus is determined by the position of the

nucleus in the crystal and by the symmetry of its environment, changes in EFG due to a phase transition appreciably affect NMR spectra. Consequently, the resonance on nuclei with spin $I > 1/2$ is a sensitive tool for fixing and investigating phase transitions and has been used frequently in specific problems. It is then obvious that in response to symmetry changes under phase transitions, a jumpwise change may occur in the quadrupole coupling constant, in the asymmetry parameter, and in the number of spectrum components (Fig. 14). Examples of such changes can be found in [177 – 179].

Phase transitions involving melting are detected especially reliably. Here, NMR often has no competitive techniques because it allows observing how a liquid phase emerges in the thinnest capillaries, in microscopic inner cavities, in thin absorption layers, and so forth.

Phase transitions in solids may change the electron configuration of resonating atoms, which induces changes in the chemical shift; these changes modify and (or) rotate the tensor of magnetic shielding. Figure 15, taken from [180], clearly shows the changes in the shielding tensor of ^{77}Se nuclei under a phase transition in ferroelectric triglycinselenate $(NH_3CH_2COO)_3H_2SeO_4$.

Other examples of using the resonances ^{77}Se, ^{1}H, and ^{2}H to study phase transitions in solids and the structure and properties of selenium compounds can be found in papers published by Lundin's group [180 – 186]. We note that much attention is currently being paid to selenium and its various compounds [187 – 189] because it is used at microscopic doses in many medicinal products, vitamins, and biologically active compounds in order to improve the functioning of various body systems in humans and animals. At the same time, however, selenium compounds — selenites and selenates — are very toxic at high dosage. But they are also quite stable in air and readily dissolve in water, which leads to considerable abundance in natural environments.

In recent paper by Gabuda, Kozlova, and Lundin [190], ^{1}H NMR techniques were used to investigate the structure of the 'guest' sublattice structure in natural zeolite — chabazite $Ca_2[Al_4Si_8O_{24}]nH_2O$; the content of zeolite water molecules varied widely ($1.5 \leqslant n \leqslant 12.8$). It was shown that if $n < 1.8$, then water molecules take part only in the ring diffusion in the vicinity of Ca^{2+} ions localized in sixfold alumosilicate rings of the structure, but if $n > 1.8$, translational diffusion of H_2O is observed. The modified mobility behavior is thought to originate with some of the exchange cations Ca^{2+} leaving ion traps and forming aquacations $[Ca(OH_2)_x]^{2+}$ inside zeolite cavities. The bimodal nature of localization of water molecules and Ca^{2+} ions occurs in the water content range from about 2 to about 8.5. A *concentration-induced phase transition* was observed to occur at $n_1 \approx 8.55$; it is connected with structural ordering in the guest subsystem formed of aquacomplexes $[Ca(OH_2)_4]^{2+}$. A similar transition at $n_2 = 10.25$ stems from the formation of $[Ca(OH_2)_5]^{2+}$ complexes. Potential barriers to the diffusion of water molecules in chabazites with various water concentrations were calculated: $U(n=6.5) = 25 \pm 4$ kJ mole^{-1}, $U(n=9.4) \approx U(n=12.0) = 32 \pm 4$ kJ mole^{-1}.

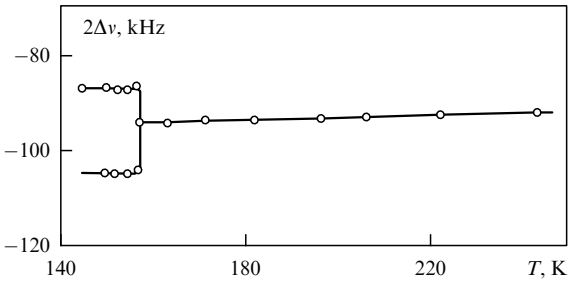

Figure 14. A phase transition in KD_2AsO_4 recorded using quadrupole NMR satellite lines of ^{2}H.

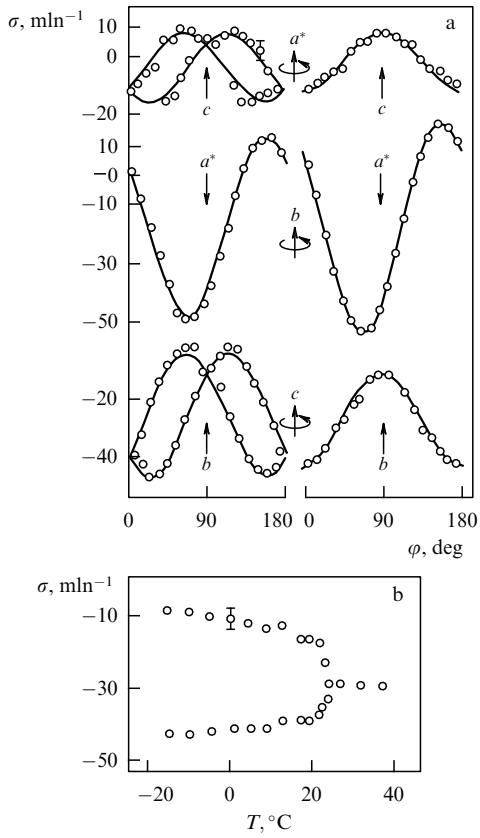

Figure 15. (a) Chemical shifts of the NMR spectrum components of ^{77}Se in a triglytsinselenate single crystal rotated around different axes and (b) splitting of spectral components as a function of temperature. On the left: temperature below the Curie point (22 °C), on the right: temperature above 22 °C.

23. NMR in solutions of inorganic salts

The properties of aqueous and alcoholic solutions of inorganic salts were studied by Zorin, Lundin et al. using the NMR of various nuclei [191 – 201]. Characteristics of solutions in the liquid state were studied in a wide range of temperatures. Furthermore, a special technique was developed for working at low temperatures, which allowed studying solutions in glassy, crystalline, and metastable liquid states, as well as transitions between these states. It is well known that practically any liquid can be transformed to a glassy state by choosing an appropriate cooling rate. In [200], paramagnetic solutions of nickel chloride and diamagnetic solutions of aluminum chloride were studied. Glasses were obtained by dipping an ampule with a solution into liquid nitrogen for 10 – 15 min. The glassified solutions were visually transparent, in contrast to polycrystalline samples obtained

by slow cooling of the same solutions. By slowly heating glassified samples, it was possible to observe an abrupt change (by a factor of several dozen!) in the width of the ^{1}H NMR spectrum at the temperature ~ 170 K resulting from the transition in the solution from a 'rigid lattice' state to a liquid (metastable) state.

In [191–193, 195, 196], proton NMR relaxation was applied to study the process of the formation of complexes in solutions of various paramagnetic salts containing divalent ions of cobalt, nickel, copper and manganese, in the presence of aprotonic diamagnetic anions Cl^-, Br^-, SO_4^{2-}. The results obtained allowed evaluating the composition of the nearest-neighbor hydration spheres of paramagnetic ions and the effect of diamagnetic cations on the composition of hydration shells and on the rate of NMR relaxation in solutions.

In [202], an NMR investigation was conducted of solutions of paramagnetic salts in liquid, supercooled, and glassified states. Activation energies of rotational mobility and relaxation times of aquacomplexes were measured, as was the mean distance between the paramagnetic ion and the nearest proton for six paramagnetic ions, including Pr^{3+}, Ce^{3+}, and Sm^{3+}.

In [195], a technique was proposed for studying the structural and dynamic parameters of systems with hydrophobic hydration in the low-temperature glass state. Studied with this technique were aqueous solutions of ethyl alcohol in the presence of lithium chloride, and a number of structural and dynamic parameters of this system were determined.

Lundin and coworkers studied the proton exchange rate in solvates of alkaline metals using ^{17}O NMR in water and methyl alcohol [197]. Currently, many papers [203–205] constructively operate with the concept of positive and negative hydration. A clearly pronounced positive hydration, under which the mobility of water molecules in the first sphere of the hydration shell of ions reduces in comparison with their mobility in free water, manifests itself in the case of singly charged ions only for Li^+ and F^-. The negative hydration producing the opposite effect on the mobility of water molecules for singly charged cations is best pronounced for Cs^+.

The ^{17}O NMR is a unique method of direct observation of the proton exchange between solvent molecules. At the same time, experiments [197] demonstrated that the ^{17}O NMR spectrum in the magnetic field of 4.7 T can be reliably recorded in various solutions with a natural abundance of the ^{17}O isotope for a limited volume of the sample.

The rates of proton exchange as functions of concentration and temperature for singly charged ions in aqueous and methanol solutions and in their deuterated analogs obtained in the project showed that the proton exchange with Li^+ ions in solutions is substantially hampered compared to solutions that contain Cs^+ ions.

The rates of proton exchange yielded by ^{14}N and ^{1}H NMR techniques were also analyzed in solutions of ammonium chloride with added hydrochloric acid [198]. The choice of ^{14}N NMR in this study proved to be preferable to using ^{15}N NMR. Especially interesting results on the proton exchange rate were obtained for the $(NH_4)^+$ ion with the isotope substitution $^1H \rightarrow {}^2H$.

24. 'Magic echo.' Time reversal in spin systems

J Waugh's monograph [51] gives a thorough enough treatment of phenomena mentioned in the title of this section. The possibility of 'time reversal' in spin systems was first pointed out by Schneider and Schmiedel [206]. It was shown that if the interval τ in the WHH-4 sequence is slightly modulated (see Fig. 5), then the mean Hamiltonian ceases to vanish in the zeroth order but is given by the expression

$$\overline{H}^0 \mathrm{d} = \frac{\delta}{\tau} H_\mathrm{d}^y .$$

We note that the coefficient δ/τ may be equal to zero but may also be negative. By varying δ, this coefficient can be changed from 1 to $-1/2$. The efficient Hamiltonian correspondingly varies in the interval

$$H_\mathrm{d}^y \leftrightarrow 0 \leftrightarrow -\frac{1}{2} H_\mathrm{d}^y .$$

Waugh's group showed in [51, 71] that there are other, simpler ways of obtaining such intervals of variation of the mean Hamiltonian. It is also possible to observe the decay of FID, which is essentially different from the one discussed above. With the mean Hamiltonian $(-1/2)\, H_\mathrm{d}^y$, the decay is twice as slow and is *reversed in time*! What can be experimentally observed then? The $\pi/2$-pulse is followed by a conventional decrease in FID; then, as the pulse sequence is imposed with the Hamiltonian $(-1/2)\, H_\mathrm{d}^y$, the process starts in the reverse direction relative to the instant $t = 0$ (Fig. 16). After the end of the pulse sequence, the system again evolves in the forward direction and a spontaneous 'magic echo' is produced because the system proceeds at this instant quite spontaneously, not being subjected to any external stimulus.

This result is rather surprising. The spin system is a thermodynamic object and is well described by a set of thermodynamic parameters: temperature, entropy, etc. Any process of relaxation of a thermodynamic system to equilibrium is accompanied by an increase in entropy and is irreversible. It appears that the main mechanism of this relaxation is spin diffusion. But diffusion is irreversible in time, i.e., substituting $-t$ for t does not reverse the process. Hence, the mechanism of generation of the magic echo is not clear at all. In fact, attempts to interpret it were considered in [10, 51, 207, 208]. Abragam and Goldman [207] wrote that 'magic pulse sequences' have a supernatural property of reversing the effective sign of the Hamiltonian, which is equivalent to time running in reverse. These authors only remark, without analyzing the physical meaning of the phenomenon of magic echo, that it does not contradict the spin temperature hypothesis.

We mention in conclusion that the magic echo is used to extract certain specific information in many experimental techniques [29, 208].

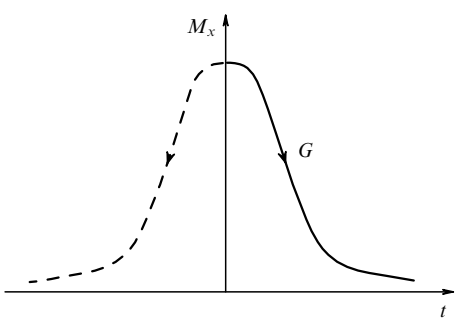

Figure 16. Transverse magnetization M_x of a sample as a function of time t.

25. NMR lineshape and the shape of spectra of other correlation functions in diamagnetic rigid-lattice crystals

The shape of NMR lines in diamagnetic crystals with a rigid lattice has attracted the attention of many researchers ever since the first experiments. It was indeed surprising that the lineshape is not Gaussian while the corresponding time response (decay of free precession signal) is oscillatory. The lineshape problem, like any many-body problem, does not have a simple theoretical solution.

Abragam [8] showed that a satisfactory description of the FID is a convolution of the rectangle with the Gauss function:

$$F(t) = \exp\left(-\frac{a^2t^2}{2}\right)\frac{\sin bt}{bt}\,. \qquad (25.1)$$

This behavior of the FID is observed in CaF_2 and other crystals [209]. According to the newest higher-accuracy measurements [210], the zeros of the FID are not equidistant and the decay curve at large times is simply exponential.

Lundin and Provotorov suggested [211] that the oscillating functions in (25.1) or those described in [210] originate in the nearest neighborhood of the selected spin, and the decaying part originates in remote spins. This model was further developed in [209, 212 – 215].

The most success so far in calculating the NMR lineshape and spectra of other correlation functions has been achieved with the self-consistent fluctuating field approximation (SCFF) [216 – 223]. Descriptions of spin dynamics in a local field whose variation in time is described by a random process trace back to the work of Anderson and Kubo [8, 224]. Provotorov et al. [225, 226] applied this approach to solve the NMR lineshape problem in a rigid lattice. The characteristics of random processes in these publications were imposed by physical arguments and self-consistent equations for temporal spin correlation functions [227 – 230] were obtained by other methods. Nonlinear integral equations derived in the SCFF approximation allowed determining the temporal correlation functions and their spectrum and producing numerical results that describe numerous experiments in homo- [218 – 220] and heteronuclear systems [221 – 223] and the shape of spectrum wings. A correct description of these wings holds special interest for the interpretation of processes of reaching equilibrium in spin systems consisting of subsystems (reservoirs) that differ greatly in resonance frequency and for the correct procedures of experimental determination of moments of the NMR spectrum (see Section 18).

26. Conclusions

This paper outlines the fundamental physical basis and describes the more important areas of application of nuclear magnetic resonance in physics and chemistry. A review is given of the most important research in the field and of applications of NMR for studying the structure, dynamics, and other properties of solids and liquids.

We discuss the main experimental NMR techniques used to study the properties of condensed systems, including relaxation NMR, the method of moments, high resolution in solids, resonance of rare isotopes, magic angle spinning, two-dimensional and multiquantum Fourier spectroscopy, and other variants of the method. NMR is characterized as one of the most important methods for studying the composition of matter, its molecular and crystalline structure, and the internal mobility of atoms and molecules in solids and liquids.

In addition to reviewing the work of the more important authors in Russia and abroad, considerable attention is paid to describing the results of research carried out by the authors of this review. It was shown, among other things, that the method of moments combined with optimized experimental techniques allows the determination of the relative coordinates of light nuclei in crystals, with an accuracy comparable to the results of neutron diffractometry. Because these are two independent physical methods, a comparison of the results obtained helps to single out a number of subtle differences in establishing internuclear distances, vibrations of nuclei around their equilibrium positions, etc.

The study of phase transitions in solids established the mechanism of spontaneous polarization in ferroelectrics of the potassium ferrocyanide family; it was shown that a structural phase transition occurs at a certain concentration of adsorbed water in chabazite zeolite; the possibility of accurately determining the transition temperature from changes in the chemical shift of spectral components was demonstrated using selenium compounds as an example.

It must be said in conclusion that writing a review that would contain a detailed description of the physical foundations of nuclear magnetic resonance and that at the same time would mention all available practical techniques is a hopeless endeavor. To make matters worse, NMR is currently going through a stage of rapid progress: many hundreds of papers appear each year reporting both enhancements and improvements of NMR methodology and practical applications of NMR for research in physics, chemistry, the medical sciences, and biology. For this reason, we paid practically no attention to such areas of NMR as the high-resolution NMR of liquids, research in the medical sciences and biology, or NMR tomography. Currently, NMR in liquids is one of the most informative methods in chemistry and as much can be said about NMR applications in biology. NMR tomography has become extremely widespread in recent years in medical sciences. Obviously, the above-mentioned technologies are in fact mature branches of science and deserve individual description.

It is also worth pointing out that NMR methods are often very useful in totally new fields of research. For instance, NMR is actively regarded now as a basis for future quantum computers that may bring about a revolution in computer technologies.

This research was supported by the RFBR grants 06-02-07008 and 06-03-32297.

References

1. Bloch F *Phys. Rev.* **70** 460 (1946)
2. Bloch F, Hansen W W, Packard M *Phys. Rev.* **69** 127 (1946)
3. Bloch F, Hansen W W, Packard M *Phys. Rev.* **70** 474 (1946)
4. Purcell E M, Torrey H C, Pound R V *Phys. Rev.* **69** 37 (1946)
5. Pople J A, Schneider W G, Bernstein H J *High-Resolution Nuclear Magnetic Resonance* (New York: McGraw-Hill Book Co., 1959) [Translated into Russian (Moscow: IL, 1962)]
6. Emsley J W, Feenney J, Sutcliffe L H *High Resolution Nuclear-Magnetic Resonance Spectroscopy* (Oxford: Pergamon Press, 1965 – 1966) [Translated into Russian (Moscow: Mir, 1968 – 1969)]
7. Bhacca N S, Williams D H *Applications of NMR Spectroscopy in Organic Chemistry* (San Francisco: Holden-Day, 1964) [Translated into Russian (Moscow: Mir, 1966)]

8. Abragam A *The Principles of Nuclear Magnetism* (Oxford: Clarendon Press, 1961) [Translated into Russian (Moscow: IL, 1063)]
9. Ostroff E D, Waugh J S *Phys. Rev. Lett.* **l6** 1097 (1966)
10. Mansfield P, Ware D *Phys. Lett.* **22** 133 (1966)
11. Brown S P, Spiess H W *Chem. Rev.* **101** 4125 (2001)
12. Smith M E, van Eck E R H *Prog. Nucl. Magn. Reson. Spectrosc.* **34** 159 (1999)
13. Laws D D, Bitter H-M L, Jerschow A *Angew. Chem. Int. Ed.* **41** 3096 (2002)
14. Eckert H *Current Opin. Solid State Mater. Sci.* **1** 465 (1996)
15. Andrew E R *Nuclear Magnetic Resonance* (Cambridge: Univ Press, 1955) [Translated into Russian (Moscow: IL, 1957)]
16. Slichter C P *Principles of Magnetic Resonance* 2nd ed. (Berlin: Springer-Verlag, 1978) [Translated into Russian (Moscow: Mir, 1981)]
17. Landau L D, Lifshitz E M *Mekhanika* (Mechanics) (Moscow: Fizmatgiz, 1958) [Translated in Englis (Oxford: Pergamon Press, 1980)]
18. Lundin A G, Fedin E I *YaMR-spektroskopiya* (NMR Spectroscopy) (Moscow: Nauka, 1986)
19. Hahn E L *Phys. Rev.* **80** 580 (1950)
20. Carr H Y, Purcell E M *Phys. Rev.* **94** 630 (1954)
21. Lowe I J, Norberg R E *Phys. Rev.* **107** 46 (1957)
22. Haeberlen U *High Resolution NMR in Solids. Selective Averadging* (New York: Academic Press, 1976); Mehring M *High Resolution NMR Spectroscopy in Solids* (Berlin: Springer-Verlag, 1976) [Translated into Russian (Moscow: Mir, 1980)]
23. Cadars S et al. *J. Phys. Chem. B* **110** 16982 (2006)
24. Fayon F et al. *J. Magn. Reson.* **179** 49 (2006)
25. Lai W C et al. *J. Am. Chem. Soc.* **128** 3878 (2006)
26. Brown S P, Emsley L *J. Magn. Reson.* **171** 43 (2004)
27. Elena B et al. *J. Am. Chem. Soc.* **127** 17296 (2005)
28. Carrington A, McLachlan A D *Introduction to Magnetic Resonance with Applications to Chemistry and Chemical Physics* (New York: Harper & Row, 1967) [Translated into Russian (Moscow: Mir, 1970)]
29. Ernst R R, Bodenhausen G, Wokaun A *Principles of Nuclear Magnetic Resonance in One and Two Dimensions* (Oxford: Oxford Univ. Press, 1987)] [Translated into Russian (Moscow: Mir, 1990)]
30. Smith S A et al. *J. Magn. Reson. A* **106** 75 (1994)
31. Bak M, Rasmussen J T, Nielsen N C *J. Magn. Reson.* **147** 296 (2000)
32. Hodgkinson P, Emsley L *Prog. Nucl. Magn. Reson.* **36** 201 (2000)
33. Edén M *Concepts Magn. Reson. A* **17A** 117 (2003)
34. Edén M *Concepts Magn. Reson. A* **18A** 1 (2003)
35. Edén M *Concepts Magn. Reson. A* **18A** 24 (2003)
36. Veshtort M, Griffin R G *J. Magn. Reson.* **178** 248 (2006)
37. Fano U *Rev. Mod. Phys.* **29** 74 (1957)
38. Kaplan J I, Fraenkel G *NMR of Chemically Exchanging Systems* (New York: Academic Press, 1980)
39. Bloembergen N, Purcell E M, Pound R V *Phys. Rev.* **73** 679 (1948)
40. Andrew E R, Bradbury A, Eades R G *Nature* **182** 1659 (1958)
41. Lowe I J *Phys. Rev. Lett.* **2** 285 (1959)
42. Andrew E R *Philos. Trans. R. Soc. London Ser. A* **299** 505 (1981)
43. Andrew E R, Bradbury A, Eades R G *Arch. Sci.* **11** 223 (1958)
44. Andrew E R, in *Progress in NMR Spectroscopy* Vol. 8 (New York: Pergamon Press, 1971)
45. Lee M, Goldburg W I *Phys. Rev.* **140** A1261 (1965)
46. Waugh J S et al. *J. Chem. Phys.* **48** 662 (1968)
47. Waugh J S, Huber L M, Haeberlen U *Phys. Rev. Lett.* **20** 180 (1968)
48. Ellett J, Haeberlen U, Waugh J *J. Am. Chem. Soc.* **92** 411 (1970)
49. Haeberlen U, Waugh J S *Phys. Rev.* **185** 420 (1969)
50. Mansfield P, in *Progress in NMR Spectroscopy* Vol. 8 (New York: Pergamon Press, 1971)
51. Waugh J S *New NMR Methods in Solid State Physics* (Cambridge: Cambridge Univ. Press, 1978) [Translated into Russian (Moscow: Mir, 1978)]
52. Pake G E *J. Chem. Phys.* **16** 327 (1948)
53. Haeberlen U, Waugh J S *Phys. Rev.* **175** 453 (1968)
54. Mehring M, Waugh J S *Phys. Rev. B* **5** 3459 (1972)
55. Pines A, Waugh J S *J. Magn. Reson.* **8** 354 (1972)
56. Mehring M et al. *J. Chem. Phys.* **54** 3239 (1971)
57. Müller R, Willsch R *J. Magn. Reson.* **21** 135 (1976)
58. Pettig M, Fenzke D, Schnabel B *Hochfrequenzspectrometer und Anwendung* (Leipzig: Akad. Wissenschaft, 1975)
59. Rhim W-K, Elleman D D, Vaughan R W *J. Chem. Phys.* **59** 3740 (1973)
60. Burum D P, Rhim W K *J. Chem. Phys.* **71** 944 (1979)
61. Griffin R G et al. *J. Chem. Phys.* **57** 2147 (1972)
62. Achlama A M, Kohlschütter U, Haeberlen U *Chem. Phys.* **7** 287 (1975)
63. Vinogradov E, Madhu P K, Vega S, in *New Techniques in Solid-State NMR* (Topics in Current Chemistry, Vol. 246, Ed. J Klinowski) (Berlin: Springer, 2004) p. 33
64. Mansfield P *Phys. Lett. A* **32** 485 (1970)
65. Mansfield P *J. Phys. C: Solid State Phys.* **4** 1444 (1971)
66. Bielecki A, Kolbert A C, Levitt M H *Chem. Phys. Lett.* **155** 341 (1989)
67. Bielecki A et al. *Adv. Magn. Reson.* **14** 111 (1990)
68. Vinogradov E, Madhu P K, Vega S *Chem. Phys. Lett.* **314** 443 (1999)
69. Vinogradov E, Madhu P K, Vega S *Chem. Phys. Lett.* **329** 207 (2000)
70. Vinogradov E, Madhu P K, Vega S *J. Chem. Phys.* **115** 8983 (2001)
71. Rhim W-K, Pines A, Waugh J S *Phys. Rev. B* **3** 684 (1971)
72. Takegoshi K, McDowell C A *Chem. Phys. Lett.* **116** 100 (1985)
73. Buszko M L, Bronnimann C E, Maciel G E *J. Magn. Reson. A* **103** 183 (1993)
74. Hohwy M, Nielsen N C *J. Chem. Phys.* **106** 7571 (1997)
75. Hohwy M et al. *Chem. Phys. Lett.* **273** 297 (1997)
76. Vega A J *J. Magn. Reson.* **170** 22 (2004)
77. Bosman L et al. *J. Magn. Reson.* **169** 39 (2004)
78. Sakellariou D et al. *Chem. Phys. Lett.* **319** 253 (2000)
79. Elena B, de Paëpe G, Emsley L *Chem. Phys. Lett.* **398** 532 (2004)
80. Lesage A et al. *J. Magn. Reson.* **163** 105 (2003)
81. Burum D P *Concepts Magn. Reson. A* **2** 213 (1990)
82. Madhu P K, Zhao X, Levitt M H *Chem. Phys. Lett.* **346** 142 (2001)
83. Pines A, Gibby M G, Waugh J S *J. Chem. Phys.* **59** 569 (1973)
84. Mehring M *Principles of High-Resolution NMR in Solids* 2nd ed. (Berlin: Springer-Verlag, 1983)
85. Hartmann S R, Hahn E L *Phys. Rev.* **128** 2042 (1962)
86. Pines A, Gibby M, Waugh J S *J. Chem. Phys.* **56** 1776 (1972)
87. Stejskal E O, Schaefer J, Waugh J S *J. Magn. Reson.* **28** 105 (1977)
88. Jeener J, in *Pulsed Magnetic and Optical Resonance. Proc. of the Ampère Intern. Summer School II, Baško Polje, Yugoslavia, 2–13 September 1971* (Ed. R Blinc) (Ljubljana: Univ., "Jožef Stefan" Inst., 1972)
89. Alla M, Lippmaa E *Chem. Phys. Lett.* **37** 260 (1976)
90. Hester R K et al. *Phys. Rev. Lett.* **36** 1081 (1976)
91. Waugh J S *Proc. Natl. Acad. Sci. USA* **73** 1394 (1976)
92. Stoll M E, Vega A J, Vaughan R W *J. Chem. Phys.* **65** 4093 (1976)
93. Rybaczewski E F et al. *J. Chem. Phys.* **67** 1231 (1977)
94. Aue W P, Bartholdi E, Ernst R R *J. Chem. Phys.* **64** 2229 (1976)
95. Ernst R R, Aue W P, Bachman P, in *Proc. of the XXth Congress AMPERE, Tallinn, 1978* (Eds E Kundla, E Lippmaa, T Saluvere) (Berlin: Springer-Verlag, 1979) p. 15
96. Schmidt-Rohr K, Spiess H W *Multidimensional Solid-State NMR and Polymers* (London: Academic Press, 1994)
97. Keeler J *Understanding NMR Spectroscopy* (Chichester: Wiley, 2005)
98. Linder M, Höhener A, Ernst R R *J. Chem. Phys.* **73** 4959 (1980)
99. Haeberlen U *Magn. Reson. Rev.* **10** 81 (1985)
100. Pines A et al., in *Proc. of the AMPERE Intern. Summer School. Pula, Yugoslavia* (1976) p. 127
101. Brunner P, Reinhold M, Ernst R R *J. Chem. Phys.* **73** 1086 (1980)
102. Reinhold M, Brunner P, Ernst R R *J. Chem. Phys.* **74** 184 (1981)
103. Warren W S, Weitekamp D P, Pines A *J. Magn. Reson.* **40** 581 (1980)
104. Warren W S, Weitekamp D P, Pines A *J. Chem. Phys.* **73** 2084 (1980)
105. Warren W S et al. *Phys. Rev. Lett.* **43** 1791 (1979)
106. Drobny G, Pines A *Philos. Trans. R. Soc. London Ser. A* **299** 585 (1981)
107. Bodenhausen G *Prog. Nucl. Magn. Reson. Spectrosc.* **14** 137 (1980)
108. Wokaun A, Ernst R R *Chem. Phys. Lett.* **52** 407 (1977)
109. Drobny G, Pines A *Chem. Symp.* **13** 49 (1979)
110. Yen Y-S, Pines A *J. Chem. Phys.* **78** 3579 (1983)
111. Sørensen O W, Levitt M H, Ernst R R *J. Magn. Reson.* **55** 104 (1983)
112. Baum J et al. *J. Chem. Phys.* **83** 2015 (1985)

113. Medek A, Harwood J S, Frydman L *J. Am. Chem. Soc.* **117** 12779 (1995)
114. Kentgens A P M *Geoderma* **80** 271 (1997)
115. Gutowsky H S, Pake G E *J. Chem. Phys.* **18** 162 (1950)
116. Lundin A G, Gabuda S P *Dokl. Akad. Nauk SSSR* **178** 641 (1968)
117. Yano S *J. Phys. Soc. Jpn.* **14** 942 (1959)
118. Ducros P *Bull. Soc. Frans Mineral Cryst.* **83** 85 (1960)
119. Gabuda S P, Lundin A G *Zh. Eksp. Teor. Fiz.* **55** 1066 (1968) [*Sov. Phys. JETP* **28** 555 (1969)]
120. Zhdanov G S *Fizika Tverdogo Tela* (Solid State Physics) (Moscow: Fizmatgiz, 1963)
121. Gabuda S P, Lundin A G *Vnutrennyaya Podvizhnost' v Tverdom Tele* (Internal Mobility in Solids) (Novosibirsk: Nauka, 1986)
122. Lundin A G, Gabuda S P *Fiz. Tverd. Tela* **10** 2516 (1968)
123. Sergeev N A, Falaleev O V, Gabuda S P *Fiz. Tverd. Tela* **11** 2247 (1969)
124. Van Vleck J H *Phys. Rev.* **74** 1168 (1948)
125. Engelsberg M, Lowe I J *Phys. Rev. B* **10** 822 (1974)
126. Lowe I J, Vollmers K W, Punkkinen M, in *Proc. of the 1st Specialized Colloque Ampere, Krakow, Poland, 1973* (Ed. J Hennel) (Krakow: Inst. of Nucl. Phys., 1973)
127. Lundin A G, Sergeev N A, Falaleev O V, in *Problemy Magnithogo Rezonansa* (Problems of Magnetic Resonance) (Ed.-in-Chief A M Prokhorov) (Moscow: Nauka, 1978) p. 226
128. Sergeev N A, Falaleev O V, Lundin A G, in *Magnitnyi Rezonans* (Magnetic Resonance) (Ed. A G Lundin) (Krasnoyarsk: Inst. Fiziki SO AN SSSR, 1977)
129. McCall D W, Hamming R W *Acta Cryst.* **12** 81 (1959)
130. Falaleev O V, Sergeev N A, Lundin A G *Kristallografiya* **19** 560 (1974)
131. Sergeev N A, Falaleev O V, Lundin A G *Kristallografiya* **23** 974 (1978)
132. Kiefer J, Wolfowitz J *Can. J. Math.* **12** 363 (1960)
133. Fedorov V V *Teoriya Optimalnogo Eksperimenta* (Theory of Optimal Experiments) (Moscow: Nauka, 1971) [Translated into English (New York: Academic Press, 1972)]
134. Hudson D J "Statistics: Lectures on elementary statistics and probability", CERN Report 63–29 (Geneva: CERN, 1964) [Translated into Russian (Moscow: Mir, 1970)]
135. Hodgkinson P *Prog. Nucl. Magn. Reson. Spectrosc.* **46** 197 (2005)
136. Bennett A E et al. *J. Chem. Phys.* **103** 6951 (1995)
137. Detken A et al. *Chem. Phys. Lett.* **356** 298 (2002)
138. Fung B M, Khitrin A K, Ermolaev K *J. Magn. Reson.* **142** 97 (2000)
139. Paëpe G D, Eléna B, Emsley L *J. Chem. Phys.* **121** 3165 (2004)
140. Ernst M, Samoson A, Meier B H *J. Magn. Reson.* **163** 332 (2003)
141. Carravetta M et al. *Chem. Phys. Lett.* **321** 205 (2000)
142. Ernst M et al. *J. Chem. Phys.* **105** 3387 (1996)
143. Ernst M, Geen H, Meier B H *Solid State Nucl. Magn. Reson.* **29** 2 (2006)
144. Gullion T, Schaefer J *J. Magn. Reson.* **81** 196 (1989)
145. Gullion T, Pennington C H *Chem. Phys. Lett.* **290** 88 (1998)
146. Chan J C C *Chem. Phys. Lett.* **335** 289 (2001)
147. Bertmer M, Eckert H *Solid State Nucl. Magn. Reson.* **15** 139 (1999)
148. Magusin P C M M et al. *J. Phys. Chem. B* **109** 22767 (2005)
149. Ladizhansky V, Vega S *J. Chem. Phys.* **112** 7158 (2000)
150. Tycko R, Dabbagh G *Chem. Phys. Lett.* **173** 461 (1990)
151. Raleigh D P, Levitt M H, Griffin R G *Chem. Phys. Lett.* **146** 71 (1988)
152. Kiihne S et al. *J. Phys. Chem. A* **102** 2274 (1998)
153. Sun B-Q et al. *J. Chem. Phys.* **102** 702 (1995)
154. Feike M et al. *J. Magn. Reson. A* **122** 214 (1996)
155. Bennett A E et al. *J. Chem. Phys.* **96** 8624 (1992)
156. Hohwy M et al. *J. Chem. Phys.* **108** 2686 (1998)
157. Nielsen N C et al. *J. Chem. Phys.* **101** 1805 (1994)
158. Dixon W T *J. Chem. Phys.* **77** 1800 (1982)
159. De Lacroix S F et al. *J. Magn. Reson.* **97** 435 (1992)
160. Shao L, Crockford C, Titman J J *J. Magn. Reson.* **178** 155 (2006)
161. Edén M, Levitt M H *J. Chem. Phys.* **111** 1511 (1999)
162. Brinkmann A, Edén M, Levitt M H *J. Chem. Phys.* **112** 8539 (2000)
163. Zaremba S K *Ann. Mat. Pura Appl.* **73** 293 (1966)
164. Conroy H *J. Chem. Phys.* **47** 5307 (1967)
165. Cheng V B, Suzukawa H H (Jr.), Wolfsberg M *J. Chem. Phys.* **59** 3992 (1973)
166. Bak M, Nielsen N C *J. Magn. Reson.* **125** 132 (1997)
167. Karney C F F *J. Mol. Graph. Model.* **25** 593 (2007)
168. Hohwy M et al. *J. Magn. Reson.* **136** 6 (1999)
169. Hodgkinson P, Sakellariou D, Emsley L *Chem. Phys. Lett.* **326** 515 (2000)
170. Zorin V E, Brown S P, Hodgkinson P *Mol. Phys.* **104** 293 (2006)
171. Zorin V E, Brown S P, Hodgkinson P *J. Chem. Phys.* **125** 144508 (2006)
172. Hodgkinson P "pNMRsim: a general simulation program for large problems in solid-state NMR", http://www.dur.ac.uk/paul.hodgkinson/pNMRsim
173. Blanton W B *J. Magn. Reson.* **162** 269 (2003)
174. Blinc R, Pintar M *J. Chem. Phys.* **35** 1140 (1961)
175. Leshe A *Izv. Akad. Nauk SSSR. Ser. fiz.* **21** 1064 (1957)
176. Gavrilova-Podol'skaya G V et al. *Izv. Akad. Nauk SSSR. Ser. fiz.* **31** 1108 (1967)
177. Bjorkstam J L, in *Advances Magnetic Resonance* (Ed. J S Waugh) (New York: Academic Press, 1973)
178. Blinc R, Žekš B *Soft Modes in Ferroelectrics and Antiferroelectrics* (Amsterdam: North-Holland, 1974) [Translated into Russian (Moscow: Mir, 1975)]
179. Cotts R M, Knight W D *Phys. Rev.* **96** 1285 (1954)
180. Moskvich Yu N et al. *Fiz. Tverd. Tela* **22** 232 (1980)
181. Sukhovskii A A et al. *Fiz. Tverd. Tela* **22** 914 (1980)
182. Lundin A G, Moskvich Yu N, Sukhovskii A A *Pisma Zh. Eksp. Teor. Fiz.* **27** 623 (1978) [*JETP Lett.* **27** 589 (1978)]
183. Lundin A G, Moskvich Yu N, Sukhovskii A A *Kristallografiya* **23** 1076 (1978)
184. Krieger A I et al. *Phys. Status Solidi A* **58** K81 (1980)
185. Nasluzova O I et al. *Solid State Sci.* **6** 1381 (2004)
186. Vinogradova I S et al. *Kristallografiya* **33** 1174 (1988) [*Sov. Phys. Crystallogr.* **33** 696 (1988)]
187. Robinson M F, in *Clinical, Biochemical, and Nutritional Aspects of Trace Elements* (Current Topics in Nutrition and Disease, Vol. 6, Ed. A S Prasad) (New York: A.R. Liss, 1982)
188. Arsenyan P et al. *Eur. J. Pharmacology* **465** 229 (2003)
189. Verma V P *Termochim. Acta* **327** 63 (1999)
190. Gabuda S P, Kozlova S G, Lundin A G *Zh. Fiz. Khim.* **79** 412 (2005) [*Russ. J. Phys. Chem.* **79** 334 (2005)]
191. Zorin V E, Lundin A G, Finkel'shtein V A *Zh. Fiz. Khim.* **72** 1409 (1998)
192. Zorin V E, Lundin A G, Finkel'shtein V A *Zh. Fiz. Khim.* **73** 1411 (1999)
193. Zorin V E, Lundin A G *J. Mol. Liquids* **91** 199 (2001)
194. Zorin V E, Lundin A G *Zh. Fiz. Khim.* **76** 1780 (2002) [*Russ. J. Phys. Chem.* **76** 1612 (2002)]
195. Zorin V E, Lundin A G *Zh. Fiz. Khim.* **76** 1784 (2002) [*Russ. J. Phys. Chem.* **76** 1616 (2002)]
196. Balandinskii A V, Zorin V E, Lundin A G *Zh. Fiz. Khim.* **78** 291 (2004) [*Russ. J. Phys. Chem.* **78** 225 (2004)]
197. Kozhura A S, Lundin A G, Falaleev O V *Zh. Fiz. Khim.* **78** 2284 (2004) [*Russ. J. Phys. Chem.* **78** 2032 (2004)]
198. Kondrasenko A A, Lundin A G *Izv. Vyssh. Uchebn. Zaved. Khim. Khim. Tekhnol.* **48** (8) 58 (2005)
199. Lundin A G et al., in *Intern. Symp. and Summer School "Nuclear Magnetic Resonance in Condensed Matter", 2nd Meeting "NMR in Life Sciences", St. Petersburg, Russia, 11–15 July 2005* Book of Abstracts (Eds V S Kasperovich, A V Komolkin) (St. Petersburg, 2005) p. 46
200. Finkel'shtein V A, Isaev I D, Lundin A G *Dokl. Akad. Nauk SSSR* **299** 877 (1988) [*Sov. Phys. Dokl.* **33** 269 (1988)]
201. Isaev I D, Lundin A G, Finkel'shtein V A *Izv. Vyssh. Uchebn. Zaved. Khim. Khim. Tekhnol.* **34** 123 (1991)
202. Lundin A G, Kozhura A S, Chichikov S A *Izv. Vyssh. Uchebn. Zaved. Khim. Khim. Tekhnol.* **48** (8) 63 (2005)
203. Samoilov O Ya *Struktura Vodnykh Rastvorov Elektrolitov i Gidratatsiya Ionov* (Structure of Aqueous Solutions of Electrolytes and Hydration of Ions) (Moscow: Izd. AN SSSR, 1957)
204. Hertz H G, Versmold H, Yoon C *Ber. Bunsenges. Phys. Chem.* **87** 577 (1983)
205. Vinogradov E V, Smirnov P R, Trostin V N *Izv. Ross. Akad. Nauk. Ser. Khim.* (6) 1186 (2003)
206. Schneider H, Schmiedel H *Phys. Lett. A* **30** 298 (1969)

207. Abragam A, Goldman M *Nuclear Magnetism*: *Order and Disorder* (Oxford: Clarendon Press, 1982) [Translated into Russian (Moscow: Mir, 1984)]
208. Cho H et al. *Phys. Rev. B* **72** 054427 (2005)
209. Fedin E I *Zh. Strukt. Khim.* **27** 60 (1986)
210. Engelsberg M, Lowe I J *Phys. Rev. B* **10** 822 (1974)
211. Lundin A A, Provotorov B N *Zh. Eksp. Teor. Fiz.* **70** 2201 (1976) [*Sov. Phys. JETP* **43** 1149 (1976)]
212. Lundin A A, Makarenko A V *Zh. Eksp. Teor. Fiz.* **87** 999 (1984) [*Sov. Phys. JETP* **60** 570 (1984)]
213. Lundin A A, Makarenko A V *Zh. Eksp. Teor. Fiz.* **102** 352 (1992) [*Sov. Phys. JETP* **75** 187 (1992)]
214. Lundin A A, Makarenko A V *Fiz. Tverd. Tela* **29** 1229 (1987) [*Sov. Phys. Solid State* **29** 702 (1987)]
215. Lundin A A *Zh. Eksp. Teor. Fiz.* **110** 1378 (1996) [*JETP* **83** 759 (1996)]
216. Zobov V E *Teor. Mat. Fiz.* **77** 426 (1988) [*Theor. Math. Phys.* **77** 1299 (1988)]
217. Zobov V E *Teor. Mat. Fiz.* **84** 111 (1990) [*Theor. Math. Phys.* **84** 751 (1990)]
218. Lundin A A, Makarenko A V, Zobov V E *J. Phys.*: *Condens. Matter* **2** 10131 (1990)
219. Zobov V E et al. *Zh. Eksp. Teor. Fiz.* **115** 285 (1999) [*JETP* **88** 157 (1999)]
220. Zobov V E, Popov M A *Zh. Eksp. Teor. Fiz.* **124** 89 (2003) [*JETP* **97** 78 (2003)]
221. Zobov V E, Lundin A A *Zh. Eksp. Teor. Fiz.* **106** 1097 (1994) [*JETP* **79** 595 (1994)]
222. Zobov V E, Lundin A A, Rodionova O E *Zh. Eksp. Teor. Fiz.* **120** 619 (2001) [*JETP* **93** 542 (2001)]
223. Zobov V E, Popov M A *Zh. Eksp. Teor. Fiz.* **127** 877 (2005) [*JETP* **100** 775 (2005)]
224. Anderson P W, Weiss P R *Rev. Mod. Phys.* **25** 269 (1953)
225. Karnaukh G E et al. *Zh. Eksp. Teor. Fiz.* **91** 2229 (1986) [*Sov. Phys. JETP* **64** 1324 (1986)]
226. Provotorov B N, Kulagina T P, Karnaukh G E *Zh. Eksp. Teor. Fiz.* **114** 967 (1998) [*JETP* **86** 527 (1998)]
227. Blume M, Hubbard J *Phys. Rev. B* **1** 3815 (1970)
228. Résibois P, De Leener M *Phys. Rev.* **152** 305 (1966)
229. Borckmans P, Walgraef D *Physica* **35** 80 (1967)
230. Borckmans P, Walgraef D *Phys. Rev.* **167** 282 (1968)